

One Dimensional Gas of Bosons with Feshbach Resonant Interactions

V. Gurarie

Department of Physics, CB390, University of Colorado, Boulder CO 80309

(Dated: November 4, 2018)

We present a study of a gas of bosons confined in one dimension with Feshbach resonant interactions, at zero temperature. Unlike the gas of one dimensional bosons with non-resonant interactions, which is known to be equivalent to a system of interacting spinless fermions and can be described using the Luttinger liquid formalism, the resonant gas possesses novel features. Depending on its parameters, the gas can be in one of three possible regimes. In the simplest of those, it can still be described by the Luttinger liquid theory, but its Fermi momentum cannot be larger than a certain cutoff momentum dependent on the details of the interactions. In the other two regimes, it is equivalent to a Luttinger liquid at low density only. At higher densities its excitation spectrum develops a minimum, similar to the roton minimum in helium, at momenta where the excitations are in resonance with the Fermi sea. As the density of the gas is increased further, the minimum dips below the Fermi energy, thus making the ground state unstable. At this point the standard ground state gets replaced by a more complicated one, where not only the states with momentum below the Fermi points, but also the ones with momentum close to that minimum, get filled, and the excitation spectrum develops several branches. We are unable so far to study this new regime in detail due to the lack of the appropriate formalism.

I. INTRODUCTION

A gas of one dimensional interacting bosons is an interesting system to study, and we have in our possession a number of techniques to study it exactly. One of the first papers to study this system, Ref. [1], demonstrated that with infinite repulsive interactions, it is equivalent to a gas of noninteracting spinless fermions. A subsequent paper Ref. [2] showed that even if the interactions are not infinite, as long as they can be approximated by short ranged delta function type interactions, the gas of interacting bosons can still be studied with the help of a method closely related to Bethe Ansatz. Its resulting behavior is in many ways equivalent to a gas of interacting fermions. In particular, two particles cannot have the same momentum when far away from each other, which is a sort of a Pauli principle for bosons. In the ground state all the momentum states below the Fermi momentum are occupied, while the rest are empty.

Subsequently it was demonstrated in Ref. [3] that the excitations of this gas around the Fermi points could be described by the effective “bosonized” theory which was later named Luttinger liquid theory. It is applicable to both systems of interacting bosons and fermions in one dimension.

Interest in such systems has been revived recently due to the emergence of new experimental techniques where the one dimensional gas of interacting bosons can be manufactured in a laboratory with ultracold bosonic atoms as its constituent particles [4]. For the first time it has become possible to study these gases experimentally.

A typical interaction between ultracold atoms is due to van der Waals forces, which are relatively short ranged compared with typical interatomic separation in a cold atom experiment, thus it is not impossible to conjecture that Bethe Ansatz techniques may be applicable to study the behavior of a gas of such atoms in one dimension. It

has also become possible to control the interactions with the help of Feshbach resonances [5]. Feshbach resonance allows to bring a pair of atoms in a resonance with a diatomic molecule, whose binding energy can be controlled by the application of magnetic field. The binding energy can be both negative, in which case the atoms will want to release their energy and form a stable molecule, or positive, in which case the molecular lifetime is finite and the molecule eventually decays into a pair of atoms.

It is well known that, in one dimension, if the molecule’s energy is negative, and if the atoms are bosons, then the system is unstable [2] and collapses into a state whose energy is negative and is proportional to the square of the number of particles. Thus the energy per particle is essentially minus infinity in the thermodynamic limit. This situation cannot be experimentally realized.

If, however, the energy of the molecule is positive, then this results in the new type of atomic gas not studied in the literature before. The study of the gas with resonant interactions is the subject of this paper.

The Hamiltonian of such a gas can be written in the following form [5]

$$H = \int dx \left[\frac{1}{2m_a} \partial_x a^\dagger \partial_x a + \frac{1}{4m_a} \partial_x b^\dagger \partial_x b + \epsilon_0 b^\dagger b + \frac{c}{2} a^\dagger a^\dagger a a + \frac{g}{\sqrt{2}} (b a^{\dagger 2} + b^\dagger a^2) \right], \quad (1)$$

where a^\dagger , b^\dagger , and a , b are bosonic atomic and molecular creation and annihilation operators. Here the interactions, given by the Feshbach term linear in b and quadratic in a , are automatically short ranged. The mass of atoms a is m_a , while the molecules b , being able to covert into two a -particles, must twice as large mass. Otherwise, Eq. (1) would violate Galilean invariance. ϵ_0 is the parameter which controls the binding energy of the molecules.

We note that the Hamiltonian Eq. (1) includes both the Feshbach g term and the delta-function interaction c term. Although often added when studying Feshbach resonant gas in higher dimensions, the c -term can be shown to be unnecessary in three dimensional space [6]. It can be absorbed into the redefinition of ϵ_0 and g . However, in one dimension the situation is different, and the delta-function term c is crucial. If the c term is omitted in Eq. (1), then there exists a real bound state of atoms with negative binding energy at all values of ϵ_0 and g . This particular situation does not arise in three dimensions. It is related to the fact that in one dimensional space (as well as in two dimensions) there exists a bound state in an arbitrary weak attractive potential. A bosonic gas with real bound state of atoms is unstable, as was discussed above.

Fortunately real atoms always repel each other at short distances, and this is encoded by the c -term in Eq. (1). This term is necessary to create a situation where real bound states are absent, while resonances, molecules with positive binding energy and finite lifetime in resonance with atomic gas, are present.

A version of the Hamiltonian Eq. (1) in higher than one dimensional space was analyzed in Ref. [7]. It is well known though that the one dimensional physics is usually quite different from its multidimensional counterpart. In one dimensional space a similar Hamiltonian was studied in Ref. [8]. However, in that paper the a -particles were spin-1/2 fermions, and the analysis presented in that paper was based on the bosonization techniques, which do not capture the excitation spectrum beyond the vicinity of the Fermi points. In this paper we study Eq. (1) exactly, and our techniques do not rely on bosonization. So we are able to obtain the exact excitation spectrum of Eq. (1).

The question of whether the techniques presented here are also suitable to study the gas of spin-1/2 fermions with resonant interactions, as the one in Ref. [8], is still open. The main difficulty seems to be the presence of the spin, which could complicate the Bethe Ansatz solution or even make it impossible to construct. We leave this question for future work.

In this paper we construct solution to the problem defined in Eq. (1) using Bethe Ansatz approach originated in Ref. [2]. These authors study Eq. (1) with $g = 0$, so we extend their techniques to the $g \neq 0$ case. It is important to stay away from real bound states of atoms in our construction, to avoid the collapse of the gas. The condition for the absence of real bound states in Eq. (1) (we will show it later in the paper) reads

$$\epsilon_0 - \frac{g^2}{c} > 0. \quad (2)$$

Thus we study Eq. (1) supplemented by this condition.

The bosonic Pauli principle for one dimensional interacting bosons of the sort studied in Ref. [2] (that is, Eq. (1) with $g = 0$) demands that no two bosons can asymptotically occupy the same state. As a result, the

bosonic system Eq. (1) at $g = 0$ can be described by the density of states $\rho(\lambda)$, where λ is the asymptotic momentum (momentum when the particles are far away from each other). The ground state corresponds to all the states up to the Fermi momentum $\pm\lambda_F$ filled, and the rest empty. The value of λ_F depends on the total density D of system (number of particles per unit length), with $D(\lambda_F)$ being a monotonously growing function of its argument. The excitation spectrum $\epsilon(\lambda)$ can also be constructed [9]. It is a monotonously growing function of λ at $\lambda > 0$, negative at $|\lambda| < \lambda_F$ and positive at $|\lambda| > \lambda_F$. It describes particle and hole excitations. In the vicinity of λ_F it can be replaced by a linear function of λ well described by the Luttinger liquid theory.

We show that the Pauli principle also holds for the Feshbach Hamiltonian Eq. (1) when applied to the atoms [10]. However, the excitation spectrum $\epsilon(\lambda)$ is more complicated than at $g = 0$. Three regimes of the resonant Hamiltonian can be identified, depending on the range of values of c . These are

$$1. c \ll \sqrt{\frac{\epsilon_0}{m_a}}, \quad 2. c \sim \sqrt{\frac{\epsilon_0}{m_a}}, \quad 3. c \gg \sqrt{\frac{\epsilon_0}{m_a}}. \quad (3)$$

In all three regimes, g is assumed to be in the range such that Eq. (2) holds.

If the total density D is small, so that λ_F is much smaller than the resonant momentum (momentum where an atom scattering off another atom with opposite and equal momentum would be in resonance with the diatomic molecule), then the density of states $\rho(\lambda)$ and the excitation spectrum $\epsilon(\lambda)$ practically coincides with that at $g = 0$ (delta function interacting Bose gas) studied in Ref. [2] and [9]. However, as the density of the gas is increased, the density of states and the excitation spectrum develop new features.

In the simplest of the three regimes, where $c \sim \sqrt{\epsilon_0/m_a}$, the excitation spectrum remains roughly similar to that of the delta function interacting Bose gas, even at higher density. However, as D is increased further, λ_F can never exceed a certain cutoff momentum $\lambda_F^{\text{cutoff}}$. As λ_F approaches the cutoff momentum, the gas accommodates the higher density by increasing its density of states $\rho(\lambda)$, as opposed to by increasing its Fermi momentum λ_F . As a function of λ , the density of states remains roughly constant in this regime. $\lambda_F^{\text{cutoff}}$ can be calculated in a closed form, but the expression for it is not simple. It can be estimated to be $\lambda_F^{\text{cutoff}} \sim m_a c$.

In the regimes of small or large c , the behavior deviates even more from that of the delta function interacting gas. As the density is increased, $\epsilon(\lambda)$ ceases to be a monotonous function of λ . Instead, it develops a local minimum above the Fermi point at a momentum such that the particles moving at this momentum are roughly at resonance with the particles in the Fermi sea. (see Fig. 10, which depicts the case where c is small. The function plotted there is $\tilde{\epsilon}(\tilde{\lambda}) = \epsilon/\lambda_F^2$ where $\tilde{\lambda} = \lambda/\lambda_F$.) This minimum cannot be captured by Luttinger liquid theory as it develops a finite distance above the Fermi

momentum and not in its immediate vicinity.

As the density is increased further, the minimum in $\epsilon(\lambda)$ gets lower. At a certain critical density D_{crit} the minimum touches zero, and above this density the minimum is now negative, Fig. 12. At this point the ground state which resulted from filling the states with λ between $-\lambda_F$ and λ_F becomes unstable and the states around the minimum also start getting filled. The actual value of the critical density can be found analytically only if c is small or $c \ll \sqrt{\epsilon_0/m_a}$, and it is given by

$$D_{\text{crit}} = \left(\frac{9m_a\epsilon_0^3}{2(c\epsilon_0 - g^2)} \right)^{\frac{1}{3}}. \quad (4)$$

The denominator of Eq. (4) is positive due to Eq. (2). The Fermi momentum of the critical gas is given by, again at small c

$$\lambda_F = (6m_a^2(c\epsilon_0 - g^2))^{\frac{1}{3}}. \quad (5)$$

The case of large c is harder to study analytically, so we do not have analytic equivalents of Eqs. (4) and (5), but on the qualitative level the behavior of the excitation spectrum is similar in both cases.

Unfortunately, we are unable to determine precise properties of the ground state and excitations once the system crosses over into this new high density regime. This is due to the fact that the equation which describes the new ground state is nonlinear, and it is not clear how to go about solving it, either analytically or numerically. So in this paper we limit ourselves with speculations about the properties of this high density state.

Which of the three regimes can be realized in the experiment depends on the properties of a particular Feshbach resonance. This is an important question, but we will not attempt to study it in this paper.

Finally, we address briefly a possible criticism which can be brought against the technique we use in this paper. This technique, taking into account merely pair-wise interactions between the atoms, does not explicitly take into account that the atoms spend some part of their time bound into molecules, and that a molecule can interact with another atom in its vicinity. We observe, however, that the density of the molecules is very small, at least in the small and large c regimes and at total densities D not exceeding too much the critical density at which the phenomena discussed in this paper take place. This is due to the fact that few atoms are in resonance with each other in the regimes of interest here. Thus interactions between the molecules, in the regimes of interest here, can be neglected. We discuss this in more detail at the end of Section III and in the Appendix E.

The rest of the paper is organized as follows. The Bethe Ansatz techniques require the knowledge of the two-body scattering matrix S . Section II is devoted to constructing the scattering theory in one dimension and applying it to Eq. (1) on the two-body level. This section can be skipped at a first reading, and its only result

important for further applications is the two-body scattering matrix Eq. (27) for the Hamiltonian Eq. (1).

In the next section III we construct Bethe Ansatz many body wavefunctions out of the two-body scattering matrix S . The procedure is fairly standard and is included for completeness.

The next section IV is devoted to the Bethe equations which allow to compute the density of states and the excitation spectrum of the Bose gas. Although standard, these equations involve the scattering phaseshift δ , related to the S -matrix as in $S = e^{2i\delta}$. The phase shift for resonantly interacting gas takes a new form which follow from Eq. (27). Thus in the remainder of that section we discuss qualitatively what behavior we can expect from δ , identifying the physically distinct large c and small c limits, depicted on Figs. 3 and 4. The functions $\theta(\lambda)$ shown on these figures is related to δ by Eq. (33).

Armed with these preliminaries we proceed to construct the ground state and the excitations of Eq. (1) in section V. It is in this section that the main results of this paper are derived and discussed.

Finally, in section VI we discuss possible structure of the ground state and excitations at densities above the critical density.

Finally, several appendices discuss technical details relevant for the material presented in this paper.

One of the most detailed discussions in the literature of the standard one dimensional interacting Bose gas, without resonances, is presented in the book Ref. [11]. Throughout this paper we extensively borrow their notations and use their results when needed.

II. ONE DIMENSIONAL SCATTERING

We begin this paper with constructing the two-body S -matrix for the Hamiltonian Eq. (1), which will be of use for the subsequent solution of the problem using Bethe Ansatz. Given a lack of discussions in the literature, it seems appropriate not only to construct it for this specific Hamiltonian, but also to discuss its general features, which is the subject of this section of the paper.

Quantum mechanics textbooks typically spend substantial time discussing scattering in three dimensional space. At the same time, scattering in one dimension is discussed only briefly. One dimensional scattering is in many regards similar to the one in three dimensions, yet there are also crucial differences.

Consider a particle in one dimension moving in a symmetric potential $U(x) = U(-x)$ which quickly vanishes at large distances, $U(x) \rightarrow 0$ if $|x| \gg r_0$,

$$-\frac{1}{2m} \frac{d^2\psi}{dx^2} + U(x)\psi = E\psi. \quad (6)$$

Here, as throughout this paper, the Planck constant \hbar is set to 1.

Typically for a problem defined in Eq. (6) we set up a transmission-reflection problem. It is defined as a so-

lution to Eq. (6) with the asymptotic behavior of $\psi(x)$ given by

$$\begin{aligned} \psi(x) &= e^{ikx} + re^{-ikx}, & x \ll -r_0, \\ \psi(x) &= te^{ikx}, & x \gg r_0. \end{aligned} \quad (7)$$

Here r and t are transmission and reflection amplitudes, with transmission and reflection probabilities given by $T = |t|^2$, $R = |r|^2$. However, for a symmetric potential, it is advantageous to set up a scattering problem defined in a way analogous to the scattering theory in 3D,

$$\begin{aligned} \psi(x) &= e^{ikx} + f_S e^{-ikx} - f_A e^{-ikx}, & x \ll -r_0, \\ \psi(x) &= e^{ikx} + f_S e^{ikx} + f_A e^{ikx}, & x \gg r_0. \end{aligned} \quad (8)$$

Here f_S and f_A are symmetric and antisymmetric scattering amplitudes (similar to the partial wave scattering amplitudes in three dimensions). It is clear that $r = f_S - f_A$, and $t = 1 + f_S + f_A$. Another way to set up a scattering problem is via an S-matrix. It is defined via a solution to Eq. (6) with the asymptotic behavior

$$\begin{aligned} \psi(x) &= e^{ikx} + S_S e^{-ikx}, & x \ll -r_0, \\ \psi(x) &= e^{-ikx} + S_S e^{ikx}, & x \gg r_0 \end{aligned} \quad (9)$$

for the scattering in the symmetric channel, and

$$\begin{aligned} \psi(x) &= -e^{ikx} + S_A e^{-ikx}, & x \ll -r_0, \\ \psi(x) &= e^{-ikx} - S_A e^{ikx}, & x \gg r_0 \end{aligned} \quad (10)$$

in the antisymmetric channel. By constructing $\psi(x) + \psi(-x)$ and $\psi(x) - \psi(-x)$ out of Eq. (8) it is easy to see that

$$f_S = \frac{S_S - 1}{2}, \quad f_A = \frac{S_A - 1}{2}. \quad (11)$$

By probability conservation the scattering matrix is unitary. As a result, the scattering matrix can be represented in terms of phase shifts

$$S_S = e^{2i\delta_S}, \quad S_A = e^{2i\delta_A}. \quad (12)$$

Another convenient representation of the scattering amplitude takes the form

$$f_S = \frac{1}{ikF_S(k^2) - 1}, \quad f_A = \frac{1}{i\frac{F_A(k^2)}{k} - 1}. \quad (13)$$

Here $F_S(k^2)$ and $F_A(k^2)$ are real functions of its argument, Taylor expandable in powers of k^2 at small k . The fact that $\text{Re}(f_{S,A}^{-1}) = -1$ is simple to establish. It follows immediately from the unitarity of the S-matrix, or from $|1 + 2f_{S,A}|^2 = 1$. It is somewhat more difficult to establish the form of $\text{Im}(f_{S,A}^{-1})$, this is done in Appendix A. All of these results closely parallel well known facts from the theory of 3 dimensional scattering (see, for example, [12]).

In this paper, we are interested in scattering of bosons, which, due to the symmetry under particle exchange, do not scatter at all in the antisymmetric channel. So, we

will not study scattering in the antisymmetric channel any further. To simplify notations, in what follows we will drop the subscripts S and A and use the notation such as $f \equiv f_S$, $S \equiv S_S$, and $F \equiv F_S$.

If we are interested in scattering at sufficiently low energy we can replace the function $F(k^2)$ by its value at zero momentum, $F(0) = -a$. Here a is usually called the scattering length. Thus the low energy scattering amplitude and S-matrix take the form

$$f = -\frac{1}{iak + 1}, \quad S = \frac{iak - 1}{iak + 1}. \quad (14)$$

It is important to keep in mind that it is not enough to take $k \ll r_0^{-1}$ for this simplification to work. In fact, the condition specifying how small k must be for Eq. (14) to work depends on the details of the potential. In all the examples of the potentials of interest in this paper, k will be taken much smaller than r_0 , yet one will often have to go far below that scale for Eq. (14) to hold. Yet, for arbitrary potential there is always some scale so that below it Eq. (14) is applicable [10].

Notice that in the limit $k \ll a^{-1}$, the scattering amplitude becomes $f = -1$, and the S-matrix is $S = -1$. This means that the transmission coefficient, $t = 1 + f$, vanishes at low energy, while the reflection coefficient $r = f = -1$. Thus we arrived at a result of utmost importance in this paper: at very low energies the scattering in an arbitrary potential in one dimension results in total reflection (with one exception, see [10]). Stated in this form, this is well known in quantum mechanics literature, see, for example, Ref. [12], problem 5 in section 25.

The scattering phase shift is related to the function F via a simple formula

$$\cot \delta = -kF(k^2) \approx ka, \quad (15)$$

where the last approximate equality holds at sufficiently low momenta. Thus at $|ka| \ll 1$, $\delta = \frac{\pi}{2}$ if a is positive and $\delta = -\frac{\pi}{2}$ if a is negative (we restrict δ to the interval $-\frac{\pi}{2}$ to $\frac{\pi}{2}$). Either way, this means that scattering at very low energies is always in the unitary limit. This result is specific to one dimension and has no equivalent in three dimensional scattering.

An important potential to study is the delta-function potential $U(x) = c \delta(x)$, where c controls its strength. It is attractive at $c < 0$ and repulsive at $c > 0$. Let us calculate scattering amplitude in this potential. It is easiest to do by first computing the phase shift. We look for a solution of the Schrödinger equation

$$-\frac{1}{2m} \frac{d^2\psi(x)}{dx^2} + c \delta(x)\psi(x) = \frac{k^2}{2}\psi(x) \quad (16)$$

in the form $\psi(x) = \cos(kx + \delta)$ for $x > 0$ and $\psi(x) = \cos(-kx + \delta)$ for $x < 0$ (this coincides with Eq. (9) up to an overall phase, and of course, in the case of delta-function, $r_0 = 0$). Direct substitution gives

$$\delta = -\arctan \frac{mc}{k}. \quad (17)$$

The scattering amplitude and S-matrix become

$$f = \frac{1}{\frac{ik}{mc} - 1}, \quad S = \frac{ik + mc}{ik - mc}. \quad (18)$$

Notice that at $k = -imc$ the scattering matrix has a pole. This pole corresponds to the bound state with the energy $E = k^2/2m = -mc^2/2$ if $c < 0$ and the potential is attractive. If, however, $c > 0$, then this pole does not correspond to the bound state and instead describes what is called in the literature a virtual bound state [12]. The existence of the bound state at $c < 0$, and its absence at $c > 0$, can also be verified by the direct substitution of $k = -imc$ into Eq. (9).

The result expressed by Eq. (18) is quite remarkable. It implies that the scattering amplitude in the delta-function potential coincides with the low energy asymptotics of the scattering amplitude in arbitrary potential, with the identification $mc = -1/a$. This is why when studying many body interacting systems with typical energies low enough for the approximation leading to Eq. (14) to hold, it is sufficient to replace the realistic interactions by the delta-function interactions, which are often easier to analyze. And this is why exact results obtained in Ref. [2, 9] for the delta-function interacting one dimensional Bose gas are applicable for the whole range of bosonic systems in one dimension regardless of their interactions.

In this paper, however, we will be interested in potentials which support a long lived quasistationary state (resonance) at positive energy $E = \epsilon_0$. A potential of this kind is depicted on Fig. 1.

At energies far below ϵ_0 , the scattering amplitude of this potential reduces to Eq. (14), just like for any other potential. However, at energies of the order ϵ_0 the scattering amplitude no longer takes the simple form Eq. (14). Indeed, the scattering amplitude must reflect in its pole structure the presence of the resonance at ϵ_0 . That means, it must have a pole at the complex value of the energy

$$\frac{k^2}{2m} = \epsilon_0 - i\Gamma/2, \quad (19)$$

where Γ is the inverse lifetime of the resonance [12].

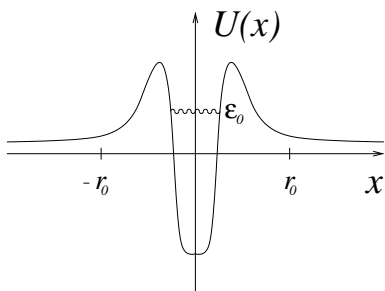


FIG. 1: A symmetric potential $U(x)$ of the typical range r_0 with the quasistationary energy level at some energy ϵ_0 .

Notice that the potential depicted on Fig. 1 can be made arbitrarily narrow (and correspondingly deep, to keep ϵ_0 at a finite value), so ϵ_0 can always be made much smaller than $1/mr_0^2$. Thus momenta of the order of $k \sim \sqrt{m\epsilon_0}$ can be made much smaller than r_0^{-1} . Yet Eq. (14) may already not apply. Instead we have to go back to a more general result Eq. (13).

To work out a typical scattering amplitude for a potential such as the one depicted on Fig. 1 is not easy. Fortunately, we do not need to work with an explicit potential. Instead, we recall that we are interested in atoms interacting via a Feshbach resonance, described by Eq. (1). Two-body version of the Feshbach Hamiltonian, sometimes referred to as a Fano-Anderson model [13] or a single level in the continuum [14], is

$$H = \frac{1}{2m} \int dx \partial_x a^\dagger \partial_x a + g [a^\dagger(0)b + b^\dagger a(0)] + \epsilon_0 b^\dagger b + c a^\dagger(0)a(0). \quad (20)$$

Notice that the numerical coefficients, present in Eq. (1) due to indistinguishability of the particles, disappeared. The Fano-Anderson Hamiltonian describes a particle, created by a^\dagger , moving a long a one dimensional line which, upon hitting the point $x = 0$, may turn into another particle, created by b^\dagger . The amplitude of this process is given by g . The b -particle does not move and has a fixed energy ϵ_0 . This particle is unstable and after some time will turn back into an a -particle which will then be free to move away from the origin. In addition, we add a delta-function repulsion from the origin for the a -particle, with strength c . As discussed in the introduction, in one dimension the presence of the delta-function repulsion makes a crucial difference (eliminates “parasitic” bound states), as we will see below.

It is not unreasonable to expect that this model describes an effective potential with long lived resonance whose energy is approximately ϵ_0 (assuming that $\epsilon_0 > 0$). The lifetime of the resonance is controlled by g . If $\epsilon_0 < 0$, then we expect that it describes a potential with a bound state. We will see below that this picture is more or less correct (although the energy of the resonance is ϵ_0 at small c only. At large c , it is at ϵ_1 , defined in Eq. (25)).

To understand the Fano-Anderson model deeper, let us compute the scattering amplitude of the a -particles. The scattering amplitude is given by the T -matrix, which is closely related to the scattering amplitude. In one dimension, this relation is given by

$$f(k) = -\frac{im}{k} T(k). \quad (21)$$

T matrix itself, for the Hamiltonian Eq. (20), can be computed diagrammatically. Leaving the details of the calculation to the Appendix B, we present the answer

$$f(k) = \left(\frac{ik}{m} \cdot \frac{\frac{k^2}{2m} - \epsilon_0}{c(\frac{k^2}{2m} - \epsilon_0) + g^2} - 1 \right)^{-1}. \quad (22)$$

First of all, we see that this scattering amplitude conforms to a general form Eq. (13) a symmetric scattering amplitude in one dimension must assume.

Second, we observe that in the absence of Feshbach term, $g = 0$, this scattering amplitude reduces to scattering in the delta-function potential, Eq. (18), as it should.

Third, we would like to study this scattering amplitude in the absence of delta-function term, $c = 0$. The scattering amplitude reduces to a simpler form

$$f_{c=0}(k) = \left(\frac{ik}{mg^2} \left(\frac{k^2}{2m} - \epsilon_0 \right) - 1 \right)^{-1}. \quad (23)$$

This indeed describes scattering via a potential with a resonance close to ϵ_0 (assuming it is positive) with the lifetime controlled by g . By analyzing the poles of Eq. (23) it is easy to see that one of them, if $g^2 \ll \epsilon_0^{\frac{3}{2}}/\sqrt{m}$, is given by

$$\frac{k^2}{2m} \approx \epsilon_0 - ig^2 \sqrt{\frac{m}{2\epsilon_0}}. \quad (24)$$

From here and from Eq. (19) we deduce that the lifetime of the resonance is inversely proportional to g^2 .

However, the scattering amplitude Eq. (23) also harbors in itself a bound state at arbitrary values of ϵ_0 . Indeed, if ϵ_0 is sufficiently large, then the energy of the bound state is simply given by $k^2/2m \approx -mg^4/2\epsilon_0^2$, where we balanced the term linear in k in Eq. (23) with -1 , neglecting the cubic in k term. If ϵ_0 is lowered until it becomes large negative, then this bound state smoothly crosses over into a more obvious bound state at $k^2/2m = \epsilon_0$, while the resonance which existed at positive values of ϵ_0 simply disappears (mathematically, its pole moves off into an unphysical part of the complex energy plane). This can be seen by finding the corresponding poles exactly.

The existence of the bound state of Eq. (20) at $c = 0$ even when ϵ_0 is positive and large can also be understood by noting that the a -particles, if their energy is below ϵ_0 , can only spend a very short time in the b -state. Their scattering will then be dominated by the second order perturbation theory where a particle jumps into a highly energetic b -state with amplitude g , and then jumps back down to one of the a -states. Such process always leads to effective attraction between a -states and the origin. Unlike the three dimensional space, in one dimension an attraction, no matter how weak, leads to a bound state. That's the bound state we observe here.

A system of one dimensional bosons with pair-wise short range interactions which support bound states is unstable and its energy per particle in the thermodynamic limit actually becomes infinitely negative. (Ref. [2]. See also discussion in the next section.) That's why we would like to study potentials when there are no bound states.

Fortunately, the full problem Eq. (20) with additional repulsive interaction $c > 0$, whose scattering amplitude is given by Eq. (22), does not have any bound states as long

as the condition Eq. (2) is fulfilled. Yet it does possess a resonance. Introducing notation

$$\epsilon_1 = \epsilon_0 - \frac{g^2}{c}, \quad (25)$$

we rewrite the scattering amplitude as in

$$f(k) = \left(\frac{ik}{mc} \frac{k^2 - 2m\epsilon_0}{k^2 - 2m\epsilon_1} - 1 \right)^{-1}. \quad (26)$$

Here $\epsilon_0 > \epsilon_1 > 0$. Indeed, at small c and g , this amplitude has a pole at $k^2/2m \approx \epsilon_0 - ig^2\sqrt{m/2\epsilon_0}$, same as Eq. (24). At large c and d , the pole is at $k^2/2m \approx \epsilon_1 - i(g^2/c^2)\sqrt{2\epsilon_1/m}$. In either of the two cases, the lifetime of the resonance is large.

We take the scattering amplitude Eq. (26) as the basic resonant scattering amplitude of interest in this paper. For future reference, we also write down the S-matrix corresponding to the amplitude Eq. (26)

$$S(k) = 2f(k) + 1 = \frac{\frac{ik}{mc} \frac{k^2 - 2m\epsilon_0}{k^2 - 2m\epsilon_1} + 1}{\frac{ik}{mc} \frac{k^2 - 2m\epsilon_0}{k^2 - 2m\epsilon_1} - 1}. \quad (27)$$

The two limits of small or large c and g , where the problem possesses a narrow resonance, have an interesting interpretation. In one of the regimes, where $c \ll \sqrt{\epsilon_0/m}$, we observe that $f(k)$ is very small almost everywhere except in the vicinity of $k = 0$ and $k^2/2m = \epsilon_0$, where $f \approx -1$. Recalling that the transmission amplitude $t = 1 + f$, we find that this regime corresponds to perfect transmission at all values of momentum except at very low momenta and at the resonance, where we have total reflection. This is the regime 1 of Eq. (3).

The other regime, $c \gg \sqrt{\epsilon_0/m}$, the regime 3 of Eq. (3), leads to $f(k) = -1$ almost everywhere except at $k^2/2m = \epsilon_1$, where $f = 0$. Thus it describes a system with total reflection at all values of energy except at resonance (which is at ϵ_1), where we have total transmission. It is not unreasonable to expect that this situation describes the transmission/reflection amplitude in case of the potential depicted on Fig. 1 (with ϵ_1 playing the role of ϵ_0 on the figure).

Whether any of the two limits is appropriate to describe experimentally observed Feshbach resonances depends on the properties of a particular resonance. This question deserves further study, but will not be discussed in this paper.

III. BETHE ANSATZ SOLUTION TO THE MANY-BODY SCHRÖDINGER EQUATION

Consider a gas of bosons moving on a line and interacting via a pair-wise interaction $U(x)$

$$-\frac{1}{2} \sum_j^N \frac{\partial^2 \psi}{dx_j^2} + \sum_{N \geq j > k \geq 1} U(x_j - x_k) = E\psi. \quad (28)$$

The wave function $\psi(x_1, x_2, \dots)$ must be symmetric under interchange of any of the coordinates. For simplicity, we set the mass of bosons to be equal to $m_a = 1$; hence the coefficient $1/2$ in front of the second derivative. Note that the reduced mass of a pair of bosons is now set at

$$m = 1/2,$$

so all the scattering formulae of the previous chapter should be understood as having this mass.

Generally speaking, for a large number of particles N and arbitrary potential $U(x)$ it is not possible to solve this equation. However, if $U(x)$ is very short ranged, then the probability that three particles simultaneously interact with one another is very low, and we can assume that only two particles interact with each other at a given time. In this case, we can use Bethe Ansatz to construct many body wave function. In what follows, we will closely follow Ref. [11] in applying Bethe Ansatz to this problem, emphasizing the differences whenever they

are present.

Usually one constructs these wave functions for the delta function interactions [11]. However, as we saw in the previous section, there are other potentials which are, on the one hand, short ranged, and on the other hand, have interesting structure. The potential depicted on Fig. 1 is one example if it is made sufficiently short ranged ($r_0 \ll 1/k$ and also much less than the typical spacing between the bosons). Even better example is given by the particles interacting via Feshbach resonance Eq. (1). Just as in Eq. (28), in what follows we take the mass of the bosons m_a in Eq. (1) to be 1, which means that the mass m in the two-body scattering matrix S is now equal to the reduced mass of the bosons, or $1/2$.

Bethe Ansatz for the many body wave function which solves Eq. (28) or Eq. (1) can be written down in the following manner. First we construct an unsymmetrized wave function $\tilde{\psi}$

$$\begin{aligned} \tilde{\psi}(x_1, x_2, \dots) &= e^{i\sum_j \lambda_j x_j}, \quad x_1 < x_2 < \dots < x_N, \\ \tilde{\psi}(x_1, x_2, \dots) &= e^{i\sum_j \lambda_j x_j} S\left(\frac{\lambda_1 - \lambda_2}{2}\right), \quad x_2 < x_1 < x_3 < \dots < x_N, \\ \tilde{\psi}(x_1, x_2, \dots) &= e^{i\sum_j \lambda_j x_j} S\left(\frac{\lambda_1 - \lambda_2}{2}\right) S\left(\frac{\lambda_1 - \lambda_3}{2}\right), \quad x_2 < x_3 < x_1 < x_4 < \dots < x_N, \\ &\dots \end{aligned} \tag{29}$$

Here $S(\lambda)$ is the scattering matrix in the potential $U(x)$, computed by solving the Schrödinger equation Eq. (6) with m being the reduced mass of the particles, $m = 1/2$. To write Eq. (29) down, we add a factor of $S((\lambda_j - \lambda_k)/2)$ for every elementary permutation between x_j and x_k ($j < k$) one needs to do to rearrange the list x_1, x_2, x_3, \dots in the order of increasing x , $x_{j_1} < x_{j_2} < \dots$.

Then we symmetrize the function $\tilde{\psi}$ to arrive at the symmetric wave function

$$\psi = \sum_P \tilde{\psi}(x_{P_1}, x_{P_2}, \dots), \tag{30}$$

where P_j represents permutations of $1, 2, \dots, N$. ψ satisfies Eq. (28) with the energy

$$E = \frac{1}{2} \sum_j \lambda_j^2. \tag{31}$$

This is proven in Appendix C. This wave function is a generalization of a standard Bethe Ansatz construction for the many body problem Eq. (28) with the delta-function potential [11].

One notable property of this wave function lies in the following: if any two λ happen to coincide, $\psi = 0$. Indeed, suppose $\lambda_j = \lambda_k$. Then it is straightforward to see

that $\tilde{\psi}(x_1, x_2, \dots)$ is antisymmetric under interchanging x_j and x_k . Two crucial properties of the S-matrix necessary to prove that are $S(0) = -1$ and $S(\lambda)S(-\lambda) = 1$, and the proof is discussed in more detail in Appendix C. Thus ψ , which is a symmetrized version of $\tilde{\psi}$, vanishes. Therefore, all λ_k must be different for the solution to the Schrödinger equation to exist.

This property of the many body one-dimensional Schrödinger equations for bosons is sometimes referred to as a bosonic ‘‘Pauli principle’’. Interacting bosons in one dimension must all have different momenta, as if they are fermions. While discussed in textbooks for delta-function potential [11], this property holds for arbitrary short ranged potentials (with one exception [10]).

Finally let us discuss the importance of the 3-body processes neglected here. We observe that in the process of checking that the wave function Eq. (30) satisfies the Schrödinger equation, we neglected the following 3-body processes. Suppose two of the coordinates, say x_j and x_k , are taken to be equal to each other. And suppose a third coordinate x_l is passed through this point. Then Eq. (30) may violate the Schrödinger equation in this range of coordinates.

When the interactions are given by delta function, then the integrability protects the 3-body processes from vi-

olating the Schrödinger equation. More generally, if the interactions are short ranged, then the weight of the wave function when two points are within the range of the interactions r_0 is negligibly small, and 3-body processes can be neglected. However, in our problem, due to the presence of the resonance, we can imagine that the wave function has a spike every time two particles in resonance approach each other. Thus a substantial part of the weight of the wave function can be at points where $x_j = x_k$.

Although one can imagine this may invalidate our solution Eq. (30) when the density D of the gas is so high that there is a finite density of the molecules in the system, we show in the Appendix E that in the interesting regimes of small c or large c , at the density of the gas around the point of instability (given by Eq. (4) at small c , for example), the density of the molecules is still sufficiently small so that we can neglect 3-body processes and rely on Eq. (30) for constructing solutions to our problem.

As the density of the gas is increased, the molecular density increases as well, and at some point the techniques discussed in this paper breaks down. However, this happens at densities well above the ones where the phenomena discussed here take place.

Ideally it would be interesting to find a model, similar in its physical properties to Eq. (1), which would be integrable so that the integrability would protect the Bethe Ansatz at all densities. Whether this is possible is not known.

IV. BETHE EQUATIONS

Not all sets of λ_j are appropriate for the wave function Eq. (30). The wave function must satisfy appropriate boundary conditions. As always, the specific form of the boundary conditions is irrelevant while it is easiest to study periodic boundary conditions. Note that if $\tilde{\psi}$ satisfies periodic boundary conditions, then ψ also satisfies them. Imposing periodic boundary conditions on $\tilde{\psi}$, we find

$$L\lambda_j + \frac{1}{i} \sum_{k \neq j} \log S \left(\frac{\lambda_j - \lambda_k}{2} \right) = 2\pi\tilde{n}_j, \quad (32)$$

where \tilde{n}_j are arbitrary integer numbers, and L is the size of the system. It is customary in the Bethe Ansatz literature to define a modified scattering phase shift θ , related to the standard phase shift $2i\delta = \log S$ in the following manner

$$\begin{aligned} \theta(\lambda) &= 2\delta(\lambda) + \pi, \quad \lambda > 0, \\ \theta(\lambda) &= -\theta(-\lambda), \quad \lambda < 0. \end{aligned} \quad (33)$$

The scattering length of the S-matrix of interest to us Eq. (26), under condition Eq. (2), is negative (this is related to the fact that the potentials of interest to us have no bound states). For negative scattering length, $\lim_{\lambda \rightarrow 0} \delta(\lambda) = -\pi/2$ (see discussion after Eq. (15)). Thus,

we find that $\theta(0) = 0$ and θ is an antisymmetric continuous function. In terms of θ , Eq. (32) becomes

$$L\lambda_j + \sum_{k=1}^N \theta \left(\frac{\lambda_j - \lambda_k}{2} \right) = 2\pi n_j, \quad (34)$$

where n_j are integers if N is odd, and n_j are half integers if N is even. These equations are called Bethe equations in the literature. They provide restriction on possible values λ_j may take. We need to solve them to find the energy spectrum of our problem.

Let us recall several useful properties of Bethe equations. It is shown in Ref. [11] that all the solutions λ_j of the equations Eq. (34) are real provided that

$$\begin{aligned} |S(\lambda)| &\leq 1 \text{ when } \text{Im } \lambda \geq 0, \\ |S(\lambda)| &\geq 1 \text{ when } \text{Im } \lambda \leq 0 \end{aligned} \quad (35)$$

Indeed, Eq. (27), together with Eq. (2), satisfies these conditions. This can be shown with some straightforward algebra. Thus, in the absence of bound states (condition expressed by Eq. (2)), all solution to the Bethe equations are real.

Second important property stems from the fact that

$$\frac{d\theta(\lambda)}{d\lambda} > 0. \quad (36)$$

This is also true courtesy of Eq. (2), as can be checked directly by examining the explicit form of the derivative of θ , given by Eq. (40). It is shown in Ref. [11] that as a consequence of positivity of derivative of θ , the solutions to the Bethe equations λ_j can be uniquely parametrized by the set of integers (half-integers) n_j . Conversely, in the presence of bound states (violation of condition Eq. (2)), the function θ is no longer monotonous, so there could be multiple solutions to Bethe equations.

Finally, it is shown in Ref. [11] that under the same condition Eq. (36) if $n_j > n_k$, then $\lambda_j > \lambda_k$. If $n_j = n_k$, then $\lambda_j = \lambda_k$. Recall that if $\lambda_j = \lambda_k$, then the wave function ψ vanishes. It follows that no two n_j may be the same.

To summarize, a set of distinct integers (half-integers) n_j , under conditions of interest to us, uniquely parametrizes the allowed momenta λ_j of the particles, and larger n_j correspond to larger λ_j .

In the remainder of this section let us analyze the behavior of θ of use in subsequent discussions in this paper.

For a delta function potential, the phase shift is given by Eq. (17). The phase θ , constructed with the help of Eq. (33) is depicted on Fig. 2. It is a monotonously increasing function, reaching π at $+\infty$ and $-\pi$ at $-\infty$.

For a resonant scattering amplitude Eq. (26), the form of the phase $\theta(\lambda)$ depends on the two possible regimes, discussed in text after Eq. (27). In the regime of small c , it is schematically depicted on Fig. 3. At $|\lambda| \lesssim \lambda_0$, where a convenient notation is introduced to be used extensively in what follows

$$\lambda_0 = \sqrt{2m\epsilon_0}, \quad \lambda_1 = \sqrt{2m\epsilon_1} = \sqrt{2m \left(\epsilon_0 - \frac{g^2}{c} \right)}, \quad (37)$$

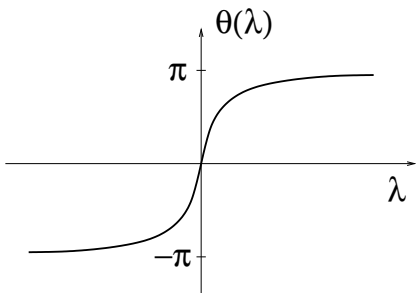


FIG. 2: A plot of $\theta(\lambda)$ for a delta function potential.

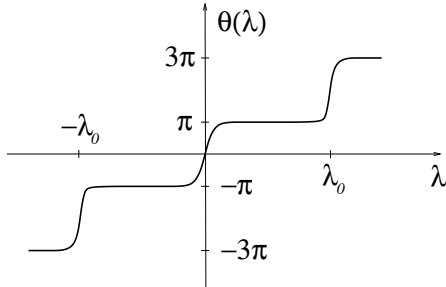


FIG. 3: A plot of $\theta(\lambda)$ for a resonant potential with scattering amplitude given by Eq. (26), and with c small. Here $\lambda_0 = \sqrt{2m\epsilon_0}$.

it closely follows the graph for $\theta(\lambda)$ for the delta function potential. However, at larger $|\lambda|$ the phase jumps by another 2π , characteristic of resonances in scattering theory (the phase shift δ jumps by π). Notice that $\theta(\pm\lambda_0) = \pm 2\pi$. This describes a situation where at almost all the energies $\theta = \pi$ or $\theta = 3\pi$, which corresponds to the total transmission. In the vicinity of $\lambda = 0$ and $\lambda = \pm\lambda_0$, the phase goes through $\theta = 0$ or $\theta = \pm 2\pi$, which is total reflection. The total change in the phase $\theta(\infty) - \theta(-\infty) = 6\pi$.

If c is large, then the phase θ is depicted on Fig. 4. The phase is either 0 or 2π almost everywhere except in the vicinity of $\lambda = \pm\lambda_1$, $\lambda_1 = \sqrt{2m\epsilon_1}$, where θ goes through π . This corresponds to total reflection almost everywhere except at energy equal to ϵ_1 . We note that at very large λ , not depicted on Fig. 4, θ subsequently increases to 3π . However, it does it very slowly and over a long interval of momenta (in the limit of very large c). We will not consider behavior of θ at such large momenta. So for our purposes $\theta(\infty) - \theta(-\infty) = 4\pi$ in this case.

Finally, we repeat that to conform with Eqs. (28) and (1), m in the preceding paragraphs should be chosen as the reduced mass of the particles there, or $m = 1/2$.

In what follows, we will need the function

$$K(\lambda) = \frac{d\theta\left(\frac{\lambda}{2}\right)}{d\lambda}. \quad (38)$$

For delta function potential, this function can be easily computed, by differentiating Eq. (17). The result is given

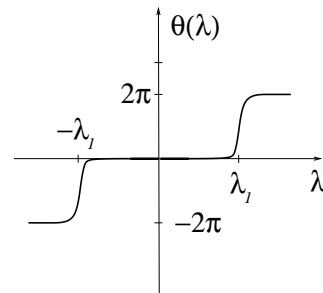


FIG. 4: A plot of $\theta(\lambda)$ for a resonant potential with scattering amplitude given by Eq. (26) and with c large. Here $\lambda_1 = \sqrt{2m\epsilon_1}$.

by

$$K(\lambda) = \frac{2c}{c^2 + \lambda^2}. \quad (39)$$

For the resonant amplitude Eq. (26) this function can also be computed directly, with the result

$$K(\lambda) = 2c \frac{\lambda^4 + 4(\lambda_0^2 - 3\lambda_1^2)\lambda^2 + 16\lambda_0^2\lambda_1^2}{(\lambda^3 - 4\lambda\lambda_0^2)^2 + c^2(\lambda^2 - 4\lambda_1^2)^2}. \quad (40)$$

This formula is not very illuminating, except if used for numerical calculations. Instead, we will concentrate on the cases of small or large c . We notice that K , being the derivative of θ depicted on Fig. 3 and Fig. 4, is zero almost everywhere except in the vicinity of $2\lambda_0$ and $2\lambda_1$ respectively. Thus, it can be well approximated by

$$K(\lambda) = \frac{2c_1}{c_1^2 + \lambda^2} + \frac{2c_2}{c_2^2 + (\lambda - 2\lambda_0)^2} + \frac{2c_2}{c_2^2 + (\lambda + 2\lambda_0)^2} \quad (41)$$

for small c , with

$$c_1 = c \frac{\lambda_1^2}{\lambda_0^2}, \quad c_2 = c \frac{\lambda_0^2 - \lambda_1^2}{2\lambda_0^2}.$$

θ , which corresponds to Eq. (41), is depicted on Fig. 3. For large c , the approximation reads

$$K(\lambda) = \frac{2c_3}{c_3^2 + (\lambda - 2\lambda_1)^2} + \frac{2c_3}{c_3^2 + (\lambda + 2\lambda_1)^2}, \quad (42)$$

where

$$c_3 = 2 \frac{\lambda_0^2 - \lambda_1^2}{c},$$

and the corresponding θ is depicted on Fig. 4.

If c is neither small nor large, a surprisingly good approximation amounts to replacing $K(\lambda)$ by its value of $\lambda = 0$, or

$$\theta(\lambda) \approx \frac{4\lambda_0^2}{c\lambda_1^2} \lambda. \quad (43)$$

This approximation, although crude and not extendable to large λ (since $\theta(\lambda) < 3\pi$), nevertheless allows to capture most features of the moderate c regime rather well, as we will see below.

V. GROUND STATE AND EXCITATIONS OF THE RESONANT BOSE GAS

To construct the ground state of the system of N particles governed by the pair-wise S-matrix S , we need to choose a set of λ_j , which satisfies Bethe equations Eq. (34) while minimizing the energy Eq. (31), with all λ_j being different. It seems reasonable that for that we need to choose n_j as small as possible. Together with the requirement that no n_j are the same, the ansatz for the ground state reads

$$n_j = -\frac{N-1}{2}, -\frac{N-1}{2} + 1, \dots, \frac{N-1}{2}. \quad (44)$$

This ansatz indeed works for the delta function potential [11]. *It will be shown below that in case of resonant scattering at small or large c , this ansatz breaks down as soon as the density of the gas exceeds a certain critical value.* Nevertheless, we would like to work out the consequences of Eq. (44) here, in the process obtaining the criteria when Eq. (44) holds.

Following Ref. [11], we introduce function $\lambda(x)$ such that $\lambda(n_j) = \lambda_j$, which satisfies, by virtue of Eq. (34), the equation

$$L\lambda(x) + \sum_{k=1}^N \theta \left(\frac{\lambda(x) - \lambda_k}{2} \right) = 2\pi x. \quad (45)$$

Differentiating this equation with respect to λ , and introducing a function

$$\rho(\lambda) = \frac{1}{L} \frac{dx}{d\lambda}, \quad (46)$$

where L is the length of the system, we find in the thermodynamic limit $N \rightarrow \infty$

$$\rho(\lambda) - \frac{1}{2\pi} \int_{-\lambda_F}^{\lambda_F} d\mu K(\lambda - \mu) \rho(\mu) = \frac{1}{2\pi}, \quad (47)$$

where K was defined in Eq. (38). Eq. (47) is called the Lieb-Liniger equation [2, 11], and K can be referred to as the kernel of this integral equation. Here $\lambda_F = \lambda_N = -\lambda_1$, is the highest momentum the particles in the ground state have. In this way, it is akin to Fermi momentum, thus the notation. $\rho(\mu)$ has the meaning of density of λ_j , with $\rho(\lambda_j) = 1/L(\lambda_{j+1} - \lambda_j)$ in the thermodynamic limit. In other words, it is the density of states per unit momentum. The total gas density can be expressed in terms of ρ as follows

$$D = \frac{N}{L} = \int_{-\lambda_F}^{\lambda_F} d\mu \rho(\mu). \quad (48)$$

By construction, $\rho(\mu)$ must be a positive function. It is shown in Ref. [11] that this implies that

$$\delta(\lambda - \mu) - \frac{1}{2\pi} K(\lambda - \mu)$$

must be a positive definite operator, with its smallest eigenvalue no smaller than $1/(2\pi\rho_{\max})$, where ρ_{\max} is the maximum value of $\rho(\lambda)$ on the interval between $-\lambda_F$ and λ_F .

A necessary condition for this operator to be positive definite is

$$\int_{-\lambda_F}^{\lambda_F} d\lambda \int_{-\lambda_F}^{\lambda_F} d\mu \left[\delta(\lambda - \mu) - \frac{1}{2\pi} K(\lambda - \mu) \right] > 0 \quad (49)$$

This is equivalent to

$$\frac{1}{\lambda_F} \int_0^{\lambda_F} d\lambda \frac{\theta(\lambda)}{\pi} < 1. \quad (50)$$

For the delta function potential whose phase θ is depicted on Fig. 2, Eq. (50) is always fulfilled no matter what λ_F . Thus, λ_F can be arbitrary. And indeed, it is possible to show that λ_F depends on D , and the bigger the total density D is, the bigger λ_F is.

However, the situation is drastically different for the resonant θ , depicted on Figs. 3 and 4. The scattering phase θ from Fig. 3 results in the relation

$$\lambda_F \lesssim \lambda_0. \quad (51)$$

At the same time, the scattering phase from Fig. 4 results in

$$\lambda_F \lesssim 2\lambda_1. \quad (52)$$

In case of moderate c , we can use Eq. (43) to find

$$\lambda_F \lesssim \frac{\pi c \lambda_1^2}{2\lambda_0^2}, \quad (53)$$

from which the estimate quoted in the Introduction follows. As a result, the Fermi momentum of the resonantly interacting Bose gas in one dimension cannot be arbitrarily large. Increasing the density of the gas D increases the Fermi momentum λ_F . However, as λ_F approaches its limit Eq. (51), Eq. (52), or Eq. (53) the density of states $\rho(\lambda)$ starts increasing very fast, and D diverges to infinity as λ approaches its upper limit. This is confirmed by numerical solution of Eq. (47). We will see below, however, that only in case of moderate c this limit can be reached. In case of small or large c , an instability develops in the ground state before the limit is reached.

The excitations above the ground state governed by the Lieb-Liniger equation Eq. (47) are controlled by the function $\epsilon(\lambda)$, which obeys

$$\epsilon(\lambda) - \frac{1}{2\pi} \int_{-\lambda_F}^{\lambda_F} d\mu K(\lambda - \mu) \epsilon(\mu) = \frac{\lambda^2}{2} - h. \quad (54)$$

Here h is the chemical potential and $\lambda^2/2 - h$ is the energy spectrum in the absence of interactions. This equation must be solved with the condition $\epsilon(\pm\lambda_F) = 0$. This condition fixes h if density D is given.

Once the function $\epsilon(\lambda)$ is known, the energy of an excitation is given by ϵ , while the momentum of this excitation is given by k , where

$$k = \lambda + \int_{-\lambda_F}^{\lambda_F} d\mu \theta \left(\frac{\lambda - \mu}{2} \right) \rho(\mu). \quad (55)$$

Positive ϵ correspond to a particle, while negative ϵ to a hole.

It is proven in the literature (see Ref. [11]) that in case where $K(\lambda)$ is a monotonously decreasing function of λ for positive λ , then the solution to Eq. (54) is a monotonously increasing function of λ for positive λ . An example of such $K(\lambda)$ is given by Eq. (39), or by the delta function potential. Then $\epsilon(\lambda) < 0$ when $|\lambda| < \lambda_F$ and $\epsilon(\lambda) > 0$ when $|\lambda| > \lambda_F$. It is consistent with the ground state where all the states with $|\lambda| < \lambda_F$ are filled, and the rest are empty. The excitations are then particle-like for $|\lambda| > \lambda_F$ or hole-like if $|\lambda| < \lambda_F$.

The situation changes drastically if $K(\lambda)$ is no longer monotonous, as in the resonant case Eq. (41) or Eq. (42). Then $\epsilon(\lambda)$ is no longer necessarily a monotonous function itself.

Eq. (47) and Eq. (54) are integral equations which in general are hard to solve analytically. In case of delta function interactions, where K is given by Eq. (39), it can only be solved in limits of very large c or very small c . The corresponding solutions are described in Appendix D.

In case of resonant interactions, where K is given by Eq. (40), we are able to find the analytic solution in two cases: the case of moderate c where we can approximate the phaseshift by Eq. (43), and in the case of small c only, where K reduces to Eq. (41). We proceed to describe the solution in these cases.

A. Ground State and Excitation of Resonant Gas: the Case of Moderate c

When $c \sim \sqrt{\epsilon_0/m_a}$, it is possible to obtain the qualitative estimate of the solution by employing the approximation Eq. (43), or

$$K(\lambda) \approx \frac{2\lambda_0^2}{c\lambda_1^2}. \quad (56)$$

Since K is a constant, solving the corresponding integral equations is straightforward. Substitution into the Lieb-Liniger equation Eq. (47) gives

$$\rho \approx \frac{1}{2\pi} \left[1 - \frac{2\lambda_0^2\lambda_F}{\lambda_1^2\pi c} \right]^{-1}. \quad (57)$$

Thus the density of states is a constant, and λ_F cannot exceed its limit given by Eq. (53). We will see below, by solving the Lieb-Liniger equation numerically, that although a crude approximation, Eq. (57) captures the main features of the density of states: it is constant and

it diverges to infinity as λ_F approaches its upper limit. The total density is approximately

$$D = \frac{\lambda_F}{\pi} \left[1 - \frac{2\lambda_0^2\lambda_F}{\lambda_1^2\pi c} \right]^{-1}. \quad (58)$$

It is equally easy to find the excitation spectrum by solving Eq. (54). We find

$$\epsilon(\lambda) \approx \frac{\lambda^2}{2} - \frac{\lambda_F^2}{2}, \quad (59)$$

where the chemical potential h is equal to

$$h \approx \frac{\lambda_F^2}{6} \left(3 - \frac{4\lambda_0^2\lambda_F}{c\pi\lambda_1^2} \right). \quad (60)$$

Thus the spectrum remains quadratic, as for the noninteracting Fermi gas. We can now find the Fermi velocity v_F by using

$$v_F \approx \left. \frac{\partial \epsilon}{\partial k} \right|_{\lambda=\lambda_F} = \frac{D}{\frac{\partial D}{\partial \lambda_F}} = \lambda_F \left[1 - \frac{2\lambda_0^2\lambda_F}{\lambda_1^2\pi c} \right] \quad (61)$$

(see Ref. [11] for derivation). Here k is the physical momentum of the excitations, given by Eq. (55). We can also find the Luttinger parameter

$$g \approx \pi \frac{\partial D}{\partial \lambda_F} = \left[1 - \frac{2\lambda_0^2\lambda_F}{\lambda_1^2\pi c} \right]^{-2}. \quad (62)$$

The Fermi velocity and the Luttinger parameter both diverge as λ_F approaches its upper limit.

B. Ground State and Excitation of Resonant Gas: the Case of Small c

When c is small, we can do far better than when c is moderate, and can obtain solution which is not just an estimate, but is correct in the limit of vanishingly small c .

As we will see in a second, in case when c is small, we only need to consider such λ_0 that $\lambda_0 \gg \lambda_F$. Under this condition, for the interval $|\lambda| \leq \lambda_F$, we can neglect the second and the third term of Eq. (41) and the function K reduces to the one for the delta function interacting potential, given by Eq. (39), with the substitution $c_1 \rightarrow c$. The corresponding Lieb-Liniger equation, given by Eq. (D1), has been studied in the literature for a long time. In particular, its solution for c being small can be found analytically. The solution is presented in Appendix D, and the answer for $\rho(\lambda)$ in the interval $-\lambda_F \leq \lambda \leq \lambda_F$ is given by Eq. (D3).

Now if we would like to know $\rho(\lambda)$ beyond this interval, we can no longer neglect the second and third term of Eq. (41). However, we can use the Lieb-Liniger equation to find $\rho(\lambda)$ for any λ by using

$$\rho(\lambda) = \frac{\lambda_F}{4\pi^2 c_1} \int_{-\lambda_F}^{\lambda_F} d\mu K(\lambda - \mu) \sqrt{1 - \frac{\mu^2}{\lambda_F^2}} + \frac{1}{2\pi}. \quad (63)$$

Taking into account that c_1 and c_2 are small, we can approximate K by a sum of three delta functions,

$$K = \delta(\lambda) + \delta(\lambda - 2\lambda_0) + \delta(\lambda + 2\lambda_0) \quad (64)$$

to find

$$\rho(\lambda) = \frac{\lambda_F}{2\pi c_1} \sqrt{1 - \frac{\lambda^2}{\lambda_F^2}}, \quad -\lambda_F \leq \lambda \leq \lambda_F, \quad (65)$$

$$\rho(\lambda) = \frac{\lambda_F}{2\pi c_2} \sqrt{1 - \frac{(\lambda - 2\lambda_0)^2}{\lambda_F^2}}, \quad 2\lambda_0 - \lambda_F \leq \lambda \leq 2\lambda_0 + \lambda_F, \quad (66)$$

and

$$\rho(\lambda) = \frac{\lambda_F}{2\pi c_2} \sqrt{1 - \frac{(\lambda + 2\lambda_0)^2}{\lambda_F^2}}, \quad -2\lambda_0 - \lambda_F \leq \lambda \leq -2\lambda_0 + \lambda_F. \quad (67)$$

Outside these three intervals within small c approximation $\rho(\lambda) = 1/(2\pi)$. The total density of the condensate coincides with its delta function value, or with Eq. (D4) with c being replaced by c_1 , or

$$D = \frac{\lambda_F^2}{4c_1}. \quad (68)$$

Now we use the same technique to find $\epsilon(\lambda)$. Within the interval $-\lambda_F \leq \lambda \leq \lambda_F$ the solution is simply given by the corresponding delta-function interaction solution, Eq. (D7). Outside this interval, we can use the approximation Eq. (64). Thus we find

$$\epsilon(\lambda) = -\frac{\lambda_F^3}{6c_1} \left(1 - \frac{\lambda^2}{\lambda_F^2}\right)^{\frac{3}{2}}, \quad |\lambda| \leq \lambda_F, \quad (69)$$

$$\epsilon(\lambda) = \frac{\lambda^2}{2} - \frac{\lambda_F^2}{4} - \frac{\lambda_F^3}{6c_1} \left(1 - \frac{(\lambda - 2\lambda_0)^2}{\lambda_F^2}\right)^{\frac{3}{2}}, \quad 2\lambda_0 - \lambda_F \leq \lambda \leq 2\lambda_0 + \lambda_F, \quad (70)$$

and

$$\epsilon(\lambda) = \frac{\lambda^2}{2} - \frac{\lambda_F^2}{4} - \frac{\lambda_F^3}{6c_1} \left(1 - \frac{(\lambda + 2\lambda_0)^2}{\lambda_F^2}\right)^{\frac{3}{2}}, \quad -2\lambda_0 - \lambda_F \leq \lambda \leq -2\lambda_0 + \lambda_F. \quad (71)$$

Outside either of the three intervals

$$\epsilon(\lambda) = \frac{\lambda^2}{2} - \frac{\lambda_F^2}{4}. \quad (72)$$

We emphasize that these formulae break down around the ends of the three appropriate intervals. We will see in the next section where we solve the Lieb-Liniger equation

numerically, that they give a rather good approximation to the actual solution.

Looking at the expressions for $\epsilon(\lambda)$ we indeed find that it is not a monotonous function of λ . In fact, it has a minimum approximately at $\lambda \approx \pm 2\lambda_0$. The minimum occurs around momenta whose particles are in resonance with Fermi sea. This is because two particles with momenta $2\lambda_0$ and 0 have a relative momentum λ_0 in their center of mass frame. Thus they are in resonance.

Moreover, it is easy to convince oneself that if λ_F is increased at a fixed λ_0 , at a certain critical value of λ_F the minimum becomes negative and the excitation spectrum becomes unstable. The critical value of the Fermi momentum when the minimum crosses zero can be also approximately found by equating Eq. (70) with zero and is given by

$$\lambda_F = (12c_1\lambda_0^2)^{\frac{1}{3}}. \quad (73)$$

Upon substituting for c_1 and expressing λ_1, λ_0 in terms of the parameters of the Hamiltonian, we find Eq. (5). Notice that this critical value of λ_F is much less than λ_0 , thus the approximation used to derive these results indeed holds. This leads to the critical value of density

$$D_{\text{crit}} = \left(\frac{9\lambda_0^4}{4c_1}\right)^{\frac{1}{3}}. \quad (74)$$

This is equivalent to Eq. (4). Above this critical density the Bose gas with resonant interactions as in Eq. (1) with c small no longer has a simple ground state described in this section of the paper, as the function $\epsilon(\lambda)$ becomes negative at momenta higher than λ_F .

To check these results, we are going to compare them with the numerical solution of the Lieb-Liniger and excitation spectrum equations.

C. Numerical Solution

For the purpose of numerics, it is advantageous to pass to dimensionless variables by the appropriate rescaling

$$\lambda = \lambda_F \tilde{\lambda}, \quad \mu = \lambda_F \tilde{\mu}, \quad c = \lambda_F \tilde{c}, \quad \epsilon = \lambda_F^2 \tilde{\epsilon}, \quad h = \lambda_F^2 \tilde{h}. \quad (75)$$

ρ does not need to be rescaled. Then the Lieb-Liniger and the energy spectrum equations become

$$\rho(\tilde{\lambda}) - \frac{1}{2\pi} \int_{-1}^1 d\tilde{\mu} \tilde{K}(\tilde{\lambda} - \tilde{\mu})\rho(\tilde{\mu}) = \frac{1}{2\pi}, \quad (76)$$

and

$$\tilde{\epsilon}(\tilde{\lambda}) - \frac{1}{2\pi} \int_{-1}^1 d\tilde{\mu} \tilde{K}(\tilde{\lambda} - \tilde{\mu})\tilde{\epsilon}(\tilde{\mu}) = \frac{\tilde{\lambda}^2}{2} - \tilde{h}. \quad (77)$$

Here \tilde{K} denotes the functions given in Eq. (41) or Eq. (42), but with $\tilde{c}_1 = c_1/\lambda_F$, $\tilde{c}_2 = c_2/\lambda_F$, $\tilde{c}_3 = c_3/\lambda_F$,

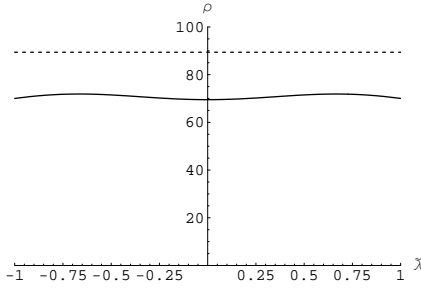


FIG. 5: $\rho(\tilde{\lambda})$ as a function of $\tilde{\lambda}$. Here K is taken from Eq. (40) with $\tilde{\lambda}_0 = 2$, $\tilde{\lambda}_1 = 1$, and $\tilde{c} = 5$. Dashed curve is the analytic estimate Eq. (57).

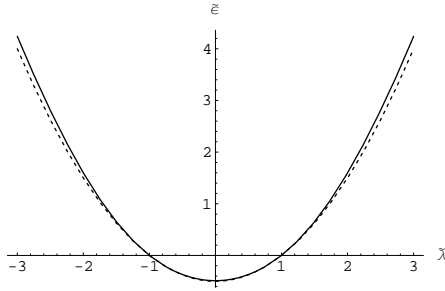


FIG. 6: $\tilde{\epsilon}(\tilde{\lambda})$ as a function of $\tilde{\lambda}$. Here K is taken from Eq. (40) with $\tilde{\lambda}_0 = 2$, $\tilde{\lambda}_1 = 1$, and $\tilde{c} = 5$. Dashed curve is the analytic estimate Eq. (59).

$\tilde{\lambda}_0 = \lambda_0/\lambda_F$, and $\tilde{\lambda}_1 = \lambda_1/\lambda_F$ replacing the variables $c_1, c_2, c_3, \lambda_0, \lambda_1$ in them.

These dimensionless equations have been solved numerically. We used a simple discretization procedure where the interval between -1 and 1 was divided into 1200 intervals, and the integrals in the equations were computed via a straightforward Newton discretization. The resulting system of linear equations was solved by inverting the kernel matrix.

1. Numerical solution for moderate c

We take $\lambda_0 = 2$, $\lambda_1 = 1$, $c = 5$. Under these conditions, the upper limit Eq. (53) for λ_F is around 2. We solve the integral equations Eq. (47) and Eq. (54) for $\lambda_F = 1.96$, close to its upper limit. Fig. 5 shows the density of states (solid line) and the analytic estimate Eq. (57) (dashed line). Although not coinciding, the estimate captures the fact that ρ is close to a constant, and that it diverges as λ_F approaches its upper limit.

Fig. 6 shows the excitation spectrum, both numerical and the analytic estimate Eq. (59) (shown as a dashed line).

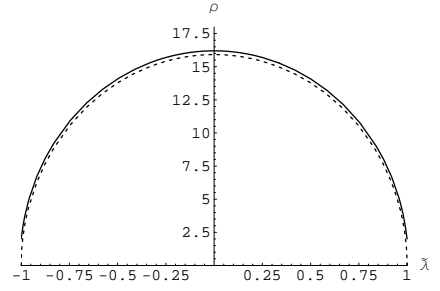


FIG. 7: $\rho(\tilde{\lambda})$ as a function of $\tilde{\lambda}$. Here K is taken from Eq. (41) with $\tilde{c}_1 = \tilde{c}_2 = 0.01$, and $\tilde{\lambda}_0 = 10$. Solid line represents numerics, while the dashed line is the analytic prediction.

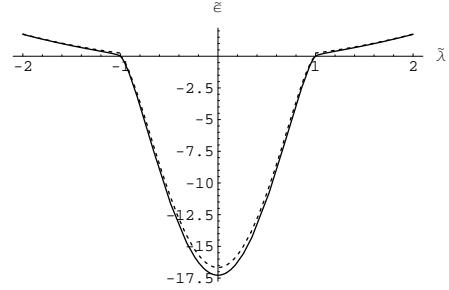


FIG. 8: $\tilde{\epsilon}(\tilde{\lambda})$. Here K is taken from Eq. (41) with $\tilde{c}_1 = \tilde{c}_2 = 0.01$, and $\tilde{\lambda}_0 = 10$. The solid curve represents numerics, and the dashed line is the analytic prediction.

2. Numerical solution for small c

We take K from Eq. (41). First, we consider the case when $\tilde{\lambda}_0 \gg 1$, or in other words the energy of the resonance λ_0 is much bigger than the Fermi momentum λ_F .

Fig. 7 presents the graph of $\rho(\tilde{\lambda})$ obtained numerically for the case when $\tilde{\lambda}_0 = 10$ and $\tilde{c}_1 = \tilde{c}_2 = 0.01$. For comparison, the analytic prediction Eq. (65) is plotted as a dashed line which generally lies slightly below the numerical line. This graph is indeed very close to Eq. (65), except at $\tilde{\lambda} = \pm 1$ where, as discussed in the Appendix D, the analytic solution breaks down.

Fig. 8 presents the graph of $\tilde{\epsilon}(\tilde{\lambda})$. The analytic predictions, which follow from Eq. (69) and Eq. (72), also work rather well. In fact, for $|\lambda| > \lambda_F$, we used Eq. (72) as opposed to a more precise Eq. (D8). Had we used this latter expression, the analytic curve would have been completely indistinguishable from the numerical line.

Finally, Fig. 9 presents the graph of $\tilde{\epsilon}(\tilde{k})$, with \tilde{k} being the rescaled momentum of the excitations, $\tilde{k} = k/\lambda_F$, where k is given by Eq. (55). For simplicity, we approximated δ in Eq. (55) by $\delta \approx \pi \text{sign}(\lambda) + \pi \text{sign}(\lambda - 2\lambda_0) + \pi \text{sign}(\lambda + 2\lambda_0)$. This graph also closely follows the analytic prediction given by Eqs. (D7), (D8), and (D9). We would like to remark that this graph shows that the excitation spectrum at $\lambda \approx \pm \lambda_F$ undergoes a sharp change in the slope. It is interesting that the Luttinger liquid theory concentrates on a tiny interval around the Fermi

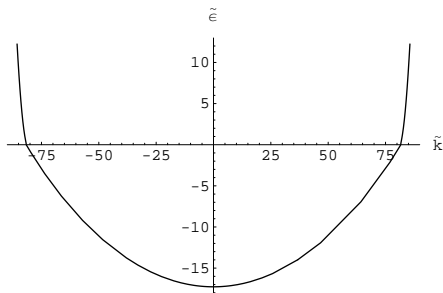


FIG. 9: $\tilde{\epsilon}(\tilde{k})$ as a function of the momentum of the excitations \tilde{k} , computed numerically. Here K is taken from Eq. (41) with $\tilde{c}_1 = \tilde{c}_2 = 0.01$, and $\tilde{\lambda}_0 = 10$.

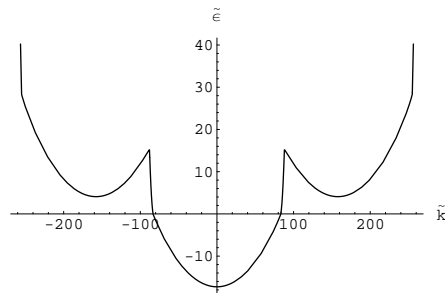


FIG. 11: $\tilde{\epsilon}(\tilde{k})$ as a function of the momentum of the excitations \tilde{k} . Here K is taken from Eq. (41) with $\tilde{c}_1 = \tilde{c}_2 = 0.01$, and $\tilde{\lambda}_0 = 3.3$.

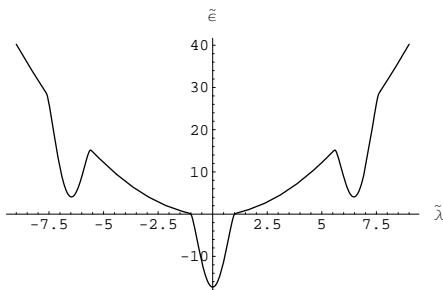


FIG. 10: $\tilde{\epsilon}(\tilde{\lambda})$ as a function of $\tilde{\lambda}$. Here K is taken from Eq. (41) with $\tilde{c}_1 = \tilde{c}_2 = 0.01$, and $\tilde{\lambda}_0 = 3.3$.

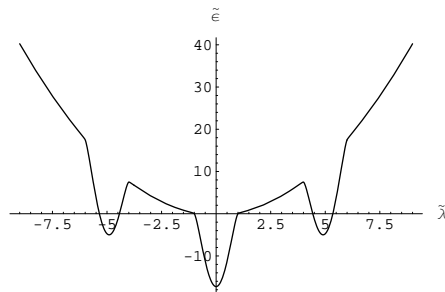


FIG. 12: $\tilde{\epsilon}(\tilde{\lambda})$ as a function of $\tilde{\lambda}$. Here K is taken from Eq. (41) with $\tilde{c}_1 = \tilde{c}_2 = 0.01$, and $\tilde{\lambda}_0 = 2.5$.

points where the spectrum can be linearized. It is clear that this theory cannot tell us anything about the spectrum away from these points (the interval where Luttinger liquid theory applies is of course so small because of the small value of \tilde{c}).

We expect that as the density of the gas is increased, or in other words, as $\tilde{\lambda}_0$ is decreased, the excitation spectrum will develop minima. At the critical value of $\tilde{\lambda}_0$, given by Eq. (73), the minimum of the spectrum will dip below zero. At $\tilde{c}_1 = 0.01$, this value is $\tilde{\lambda}_0 \approx 2.89$. We solve the integral equations numerically at $\tilde{\lambda}_0 = 3.3$.

The density of states in the interval $-1 \leq \tilde{\lambda} \leq 1$ remains basically unchanged, as predicted. Let us now look at the excitation spectrum. We present here both the spectrum as a function of $\tilde{\lambda}$, and as a function of \tilde{k} , see Fig. 10 and 11. It differs drastically from that on Fig. 8. Namely it developed an additional minimum at $\lambda \approx 2\lambda_0$. We only plot numerical curves on these graphs as the analytic curves given by Eqs. (69), (70), (71), and (72) are almost indistinguishable from the numerical ones.

We can understand the appearance of a minimum at $\lambda = 2\lambda_0$ by noticing that the particles which move at $\lambda = 2\lambda_0$ scatter off the bulk of the Fermi sea exactly at resonance. Therefore, these particles try to form bound states with those in the Fermi sea and the resulting bosons then Bose condense.

Now let us look the spectrum at $\tilde{\lambda}_0 = 2.5$. The density of states is again not much different from that on Fig. 7, but the spectrum changes again, and is shown on Fig. 12

and Fig. 13. Remarkably, the spectrum develops areas where $\epsilon < 0$. By filling up the states where ϵ is negative, it is possible to lower the energy of the system compared to that of the ground state. Therefore, the state discussed in this section becomes unstable, and is no longer the ground state in this regime. It can be checked numerically that this instability develops roughly at $\tilde{\lambda}_0 \approx 2.9$, just as predicted analytically. This is why we refer to the state where only the states between $-\lambda_F$ and λ_F are filled as “simple ground state”. At sufficiently high density of the gas the ground state changes.

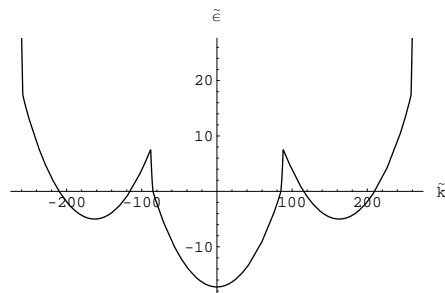


FIG. 13: $\tilde{\epsilon}(\tilde{k})$ as a function of the momentum of the excitations \tilde{k} . Here K is taken from Eq. (41) with $\tilde{c}_1 = \tilde{c}_2 = 0.01$, and $\tilde{\lambda}_0 = 2.5$.

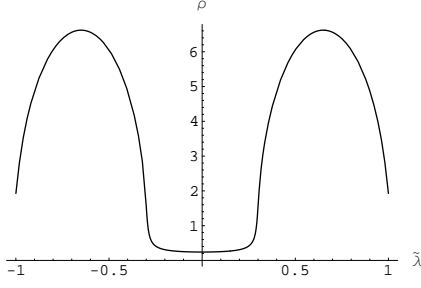


FIG. 14: The density of states $\rho(\tilde{\lambda})$ for the case of large c , Eq. (42). $\tilde{c}_3 = 0.01$, $\tilde{\lambda}_1 = 0.65$.

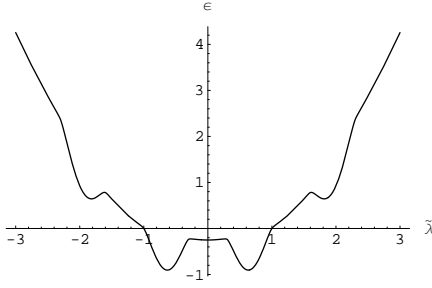


FIG. 15: $\tilde{\epsilon}(\tilde{\lambda})$ as a function of $\tilde{\lambda}$. Here K is taken from Eq. (42) with $c_3 = 0.01$, and $\lambda_1 = 0.65$.

3. Numerical solution at large c

If c is very large, then the kernel K can be taken from Eq. (42). We are not able to find an analytical solution for this case, and present the numerical solution. It is qualitatively similar to the one at small c , although it has several new features.

We take $\tilde{c}_3 = 0.01$, and present numerical solution for $\tilde{\lambda}_1 = 0.65$, above the instability, and for $\tilde{\lambda}_1 = 0.55$, below the instability. $\tilde{\lambda}_1$ can generally take values smaller than appropriate values of λ_0 at small c because of the condition Eq. (52) as compared to Eq. (51). The density of states at $\lambda_1 = 0.65$ is shown on Fig. 14. Notice it is quite different from the analytically understood case of small c , depicted on Fig. 7.

As far as the energy spectrum, it is depicted on Fig. 15. It has minima similar to the ones on Fig. 9. In addition, not only particles, but also holes have nonmonotonous spectrum. Fig. 16 shows the same spectrum, but as a function of a physical momentum k .

Fig. 17 and 18 show the excitation spectrum for $\lambda_0 = 0.55$. Now the spectrum is unstable.

VI. BEYOND THE SIMPLE GROUND STATE

If the density of gas is increased beyond the critical density, at small c or at large c , then we can no longer use the Lieb-Liniger and excitation integral equations Eqs. (47) and (54). Instead, we can take a different path.

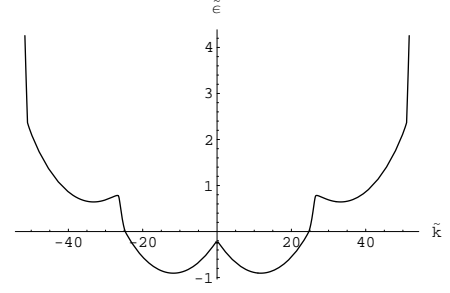


FIG. 16: $\tilde{\epsilon}(\tilde{k})$ as a function of the physical momentum \tilde{k} . Here K is taken from Eq. (42) with $\tilde{c}_3 = 0.01$, and $\tilde{\lambda}_1 = 0.65$.

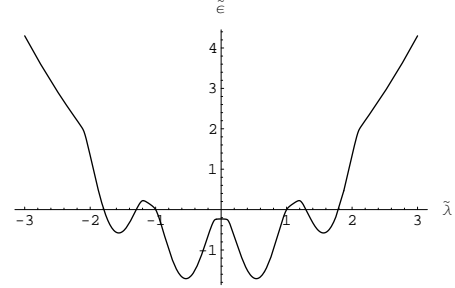


FIG. 17: $\tilde{\epsilon}(\tilde{\lambda})$ as a function of $\tilde{\lambda}$. Here K is taken from Eq. (42) with $\tilde{c}_3 = 0.01$, and $\tilde{\lambda}_1 = 0.55$.

The problem we confront is that above the critical density we no longer know which states are filled and which states are empty in the ground states. We can circumvent this problem by writing down the zero temperature version of the Yang-Yang equation [11], which looks like

$$\epsilon(\lambda) - \frac{1}{4\pi} \int_{-\infty}^{\infty} d\mu K(\lambda - \mu) [\epsilon(\mu) - |\epsilon(\mu)|] = \frac{\lambda^2}{2} - h. \quad (78)$$

This equation has to be solved at a given chemical potential h . Once its solution is known, we know that the particles states are those where $\epsilon(\lambda) > 0$, while the hole states are where $\epsilon(\lambda) < 0$. We can now determine the

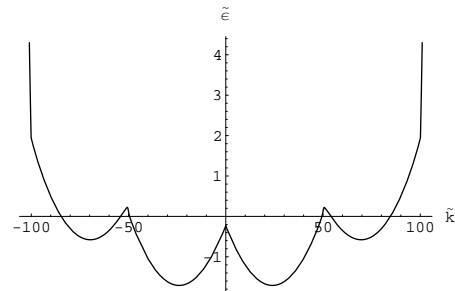


FIG. 18: $\tilde{\epsilon}(\tilde{k})$ as a function of the physical momentum \tilde{k} . Here K is taken from Eq. (42) with $\tilde{c}_3 = 0.01$, and $\tilde{\lambda}_1 = 0.65$.

density of states by solving

$$\rho(\lambda) - \frac{1}{4\pi} \int_{-\infty}^{\infty} d\mu K(\lambda - \mu)\rho(\mu) [1 - \text{sign } \epsilon(\lambda)] = \frac{1}{2\pi}. \quad (79)$$

In case of low density resonant gas it is easy to solve Eq. (78) as the integration there is effectively over the region where $\epsilon(\lambda)$ is negative. In those simple cases, we know that $\epsilon(\lambda)$ is negative only for $-\lambda_F \leq \lambda \leq \lambda_F$ and Eq. (78) reduces to Eq. (54). But above the critical density, it is not at all clear how to solve these equations, either analytically or numerically. Numerically, any naive scheme one could use to solve Eq. (78) becomes unstable. For example, trying to find the solution by neglecting the integral in Eq. (78) first, and then taking it into account via iterations, immediately leads to an instability and a solution which quickly diverges with each successive iteration. In fact, it is proven in Ref. [11] that solving Eq. (78) by iterations works. However, their proof essentially uses the monotonicity of $K(\lambda)$ for $\lambda > 0$, that is, it breaks down for resonant interactions.

It is intuitively clear that above the critical density the single particle states whose momentum λ falls into the areas of negative $\epsilon(\lambda)$, such as on Fig. 12, will be filled. But all of those states cannot be filled. Otherwise, the analog of the condition Eq. (49) (which is the very same condition, except the regions of integration are now over where $\epsilon(\lambda)$ is negative) would be violated. Unfortunately, it is not clear how to improve this intuition and make it more quantitative.

Solving Eq. (78) and studying the resonant gas above the critical density will be left for future work.

VII. CONCLUSIONS AND OUTLOOK

We presented the technique for solving the problem of one dimensional resonantly interacting Bose gas exactly. With the Hamiltonian given by Eq. (1), supplemented by the condition Eq. (2), we found the solution analytically for small c , or $c \ll \sqrt{\epsilon_0/m_a}$, at density below the critical density Eq. (4). In particular, we found the exact excitation spectrum, given by Eqs. (69), (70), (71), and (72). The excitation spectrum is not monotonous and has minima above the Fermi momentum. A typical excitation spectrum, as a function of asymptotic momentum λ is shown on Fig. 10. An excitation spectrum as a function of a physical momentum of a quasiparticle is shown on Fig. 11. Above the critical density the solution we found becomes unstable and we were not able to find a stable solution in this regime. These features of the solution to the resonantly interacting gas remain valid at large c as well, as confirmed by numerical solutions of the Bethe Ansatz equations.

The minima in the excitation spectrum should be easily observable experimentally, if such a one dimensional gas is realized in a laboratory. Indeed, at any finite temperature, one should observe low energy excitations far

above the Fermi momentum. These could be observed in a time of flight experiment.

At $c \sim \sqrt{\epsilon_0/m_a}$, the excitation spectrum does not develop minima and the gas can be described by the Luttinger liquid theory. However, in one difference from the nonresonantly interacting Bose gas, its Fermi momentum λ_F can never exceed a certain cutoff momentum in this regime. The increased density of gas is accommodated by the ever increasing density of states, as opposed to the Fermi momentum.

In view of the possible future experiments, it is important to generalize the theory presented here to nonzero temperature. This would be straightforward to do by employing the appropriate Yang-Yang equation.

The nature of the phase above the critical density for large or small c remains undetermined, and should be another subject of future work.

A major limitation of the technique used in this paper is the neglect of three-body processes. Although justified in the relatively low density regimes considered here, a major technical improvement would involve coming up with a technique where this deficiency is absent. Perhaps an integrable version of Eq. (1) can be formulated or some other technique can be proposed. Whether this is possible to do is currently not clear. In the absence of exact techniques, bosonization remains the only alternative if one wants to study high density regimes where the density of molecules is supposed to be of the order of the density of atoms.

Finally, an interesting generalization of the work presented here would be to study a gas of fermions resonantly interacting and confined to one dimension. The main difficulty which will have to be overcome is that fermions carry spin, the S -matrix becomes a real matrix in the spin space, and the Bethe Ansatz techniques become much more technically involved than in the case considered in this paper.

Acknowledgments

The author is grateful to A. Tselvik and R. Konik for useful comments at the beginning of this work, and to L. Radzihovsky and D. Sheehy for many discussions. This work was supported by the NSF grant DMR-0449521.

APPENDIX A: LOW ENERGY ONE DIMENSIONAL SCATTERING

We would like to derive formulae Eq. (13). Closely following Ref. [12], we observe that

$$|S_{S,A}|^2 = |1 + 2f_{S,A}|^2 = 1.$$

It follows from here that

$$2 + \frac{1}{f_{S,A}} + \frac{1}{f_{S,A}^*} = 0,$$

and thus, $\text{Re } f_{S,A}^{-1} = -1$. We deduce

$$f_{S,A} = \frac{1}{i\tilde{F}_{S,A}(k) - 1},$$

where $\tilde{F}_{S,A}$ is a function of momentum k , real when k is real. Notice that

$$\cot \delta_{S,A} = -\tilde{F}_{S,A}(k).$$

Next we would like to analyze the behavior of \tilde{F} at very small momenta. For that we need to study the Schrödinger equation at small energy. We observe that it is possible to split the range of x into several intervals. In the interval $-r_0 \lesssim x \lesssim r_0$, we can neglect energy to find the Schrödinger equation

$$-\frac{1}{2m} \frac{\partial^2 \psi}{\partial x^2} + U(x)\psi = 0, |x| < r_0 \quad (\text{A1})$$

This equation must be solved with the boundary conditions $\psi(0) = 1$, $\frac{d\psi(0)}{dx} = 0$ for symmetric amplitude, and with the conditions $\psi(0) = 0$, $\frac{d\psi(0)}{dx} = 1$ if we study antisymmetric amplitude.

In the interval $r_0 \lesssim |x| \lesssim 1/k$, we neglect the potential and the energy to arrive at

$$-\frac{1}{2m} \frac{\partial^2 \psi}{\partial x^2} = 0.$$

Its solution is $\psi = c_1 + c_2 x$. The constants c_1 and c_2 can be determined by matching this solution with the solution to Eq. (A1) in the range of $|x| \sim r_0$. The crucial point is that they are energy independent. They of course depend on whether we are looking at symmetric or antisymmetric amplitude.

Finally in the range $|x| \gtrsim 1/k$, the potential (but not the energy) can be neglected, and the Schrödinger equation reduces to

$$-\frac{1}{2m} \frac{\partial^2 \psi}{\partial x^2} = \frac{k^2}{2m} \psi.$$

The solution to this reads $A \cos(kx + \delta_S)$ in the symmetric case or $A \sin(kx + \delta_A)$ in the antisymmetric case, if $x \gtrsim 1/k$ and their symmetric (antisymmetric) reflection if $x \lesssim -1/k$. Extending it to $|x| < 1/k$, we find $\cot \delta_S = -kc_1/c_2$. Thus $\tilde{F}_S = kc_1/c_2$ at small k , and we arrive at

$$f_S = \frac{1}{ikF_S(k^2) - 1},$$

where $F_S(k) = \tilde{F}_S(k)/k$, and $F_S(0)$ is finite. Quite analogously, taking the asymptotics $A \sin(kx + \delta_A)$, we find $k \cot \delta_A = c_2/c_1$, leading to

$$f_A = \frac{1}{\frac{i}{k}F_A(k^2) - 1},$$

where $F_A(0)$ is finite.

Finally, we observe that for purely imaginary k the scattering amplitude must be real. For that the functions F_S and F_A must be even functions of momentum k , which explains why they are the functions of k^2 .

APPENDIX B: T -MATRIX CALCULATION OF THE SCATTERING AMPLITUDE

We would like to calculate the T -matrix of the a -particles described by Eq. (20). The definition of T -matrix is given in many textbook, see, for example, Ref. [15]. It is basically the exact Green's function with free Green's function subtracted and external legs amputated.

We note that the free Green's function is given by

$$G_0(E; k) = \frac{1}{E - \frac{k^2}{2m} + i0},$$

and the Green's function of b -particles is

$$D(E) = \frac{1}{E - \epsilon_0 + i0}.$$

The T -matrix is given by the geometric series

$$T = \tilde{c} + \tilde{c}\tilde{G}\tilde{c} + \dots = \frac{\tilde{c}}{1 - \tilde{G}\tilde{c}}.$$

Here \tilde{G} represents trace of the Green's function

$$\tilde{G} = \int_{-\infty}^{\infty} \frac{dk}{2\pi} \frac{1}{E - \frac{k^2}{2m} + i0} = -i\sqrt{\frac{m}{2E}},$$

and \tilde{c} is

$$\tilde{c} = c + gDg.$$

Thus the T -matrix is

$$T = \frac{c + gDg}{1 - \tilde{G}(c + gDg)} = \left(\frac{E - \epsilon_0}{c(E - \epsilon_0) + g^2} - \tilde{G} \right)^{-1}.$$

Upon substituting $E = k^2/2m$ and using Eq. (21) we get Eq. (22).

APPENDIX C: BETHE ANSATZ FOR THE MANY-BODY WAVE FUNCTION

We would like to discuss why Eq. (30) solves the appropriate Schrödinger equation. The proof is known from the studies of Bethe Ansatz. We are not going to present a mathematical proof, but merely list the reasons why this is the case.

If $x_1 \neq x_2 \neq \dots \neq x_n$, then clearly this wave function solves the Schrödinger equation by construction, with the energy given by Eq. (31).

Let us now take x_j close to x_k so that there are no other particles between these two. The terms in Eq. (30) can be split into pairs which differ by exchanging x_j and x_k . Let's take one such pair. Then if $x_j < x_k$, the wave function which includes the sum over this pair will be proportional to

$$\psi \sim e^{i\lambda_1 x_j + i\lambda_2 x_k} + e^{i\lambda_1 x_k + i\lambda_2 x_j} S\left(\frac{\lambda_1 - \lambda_2}{2}\right),$$

where λ_1 and λ_2 are two momenta which x_j and x_k get multiplied by in the exponential in each of this pair of terms. If, however, $x_j > x_k$, then the wave function is proportional to

$$\psi \sim e^{i\lambda_1 x_j + i\lambda_2 x_k} S\left(\frac{\lambda_1 - \lambda_2}{2}\right) + e^{i\lambda_2 x_j + i\lambda_1 x_k}.$$

Introducing relative coordinates

$$R = \frac{x_j + x_k}{2}, \quad r = x_j - x_k,$$

$$\lambda = \frac{\lambda_1 - \lambda_2}{2}, \quad \Lambda = \lambda_1 + \lambda_2,$$

we find

$$\psi \sim e^{\Lambda R} (e^{i\lambda r} + S(\lambda)e^{-i\lambda r}),$$

for $r < 0$ and

$$\psi \sim e^{\Lambda R} (e^{-i\lambda r} + S(\lambda)e^{i\lambda r}),$$

for $r > 0$. This coincides with the definition of the scattering matrix Eq. (9). So Eq. (30) indeed solves the Schrödinger equation even when the particles pass through each other.

Now let us show that if $\lambda_j = \lambda_k = \lambda$, then $\tilde{\psi}$, defined in Eq. (29), is antisymmetric under the exchange of x_j and x_k . Indeed, suppose that $x_j < x_k$. Then once x_j and x_k are exchanged, we need to bring x_k through all the particles separating x_j and x_k until it occupies the position x_j normally occupies. At the same time x_j should be brought back to the position it normally occupies. Each exchange of x_k with the particles x_l in between brings $S\left(\frac{\lambda_l - \lambda}{2}\right)$, where l labels these particles. Each exchange of x_j brings the factor $S\left(\frac{\lambda_l - \lambda}{2}\right)$. Finally, an exchange of x_j and x_k brings the factor $S(0)$. Thus $\tilde{\psi}$, where x_j and x_k were exchanged, differs from $\tilde{\psi}$ before the exchange, by the factor of

$$S(0) \prod_l S\left(\frac{\lambda - \lambda_l}{2}\right) S\left(\frac{\lambda_l - \lambda}{2}\right) = -1. \quad (\text{C1})$$

Here the product is over all the particles between x_j and x_k . And indeed, $S(\lambda)S(-\lambda) = 1$, as follows directly from the form

$$S(\lambda) = \frac{i\lambda F(\lambda^2) + 1}{i\lambda F(\lambda^2) - 1},$$

which follows from Eq. (13). At the same time $S(0) = -1$, as follows from the same relation.

This important property, from which the bosonic ‘‘Pauli principle’’ immediately follows, has one notable exception. Take the scattering amplitude Eq. (27) and set $\epsilon_1 = 0$. This corresponds to $\epsilon_0 - g^2/c = 0$, or in other word, to the situation where there is a bound state exactly at zero energy. Then, as can be easily checked, $S(0) = 1$. Thus in these circumstances there is no bosonic ‘‘Pauli principle’’. Fortunately, this only happens when the condition of interest to us, Eq. (2), is violated.

APPENDIX D: GROUND STATE AND EXCITATIONS OF THE BOSE GAS WITH DELTA FUNCTION INTERACTIONS

Consider the Bose gas Eq. (28) with repulsive two body potential $U(x) = c \delta(x)$ ($c > 0$), and with total density (number of particles per unit length) D .

The solution to this problem can be found by solving the equations of Bethe Ansatz. Generally this involves solving integral equations which can only be solved numerically. The limits of very strong or very weak interactions can nevertheless be solved analytically. We present the solutions here.

If the interaction is very strong ($c \gg D$), then the kernel of the integral equation, Eq. (39) vanishes. The Lieb-Liniger equation can be solved elementary, to give

$$\rho(\lambda) = \frac{\lambda}{2\pi}.$$

The total density of the gas is then

$$D = \int_{-\lambda_F}^{\lambda_F} d\mu \rho(\mu) = \frac{\lambda_F}{\pi}.$$

The Fermi velocity of the gas is given by (see Ref. [11])

$$v_F = \frac{D}{\frac{\partial D}{\partial \lambda_F}} = \lambda_F,$$

and the excitation spectrum is given by

$$\epsilon(\lambda) = \frac{\lambda^2}{2} - h,$$

where h is the chemical potential.

Thus the Bose gas with strong repulsions is equivalent to a non-interacting Fermi gas, as is well known [1].

A somewhat more nontrivial regime is the one where the interaction strength is weak compared to density, $c \ll D$. Then the Bethe Ansatz equations can be approximately solved in the following way.

First, consider the Lieb-Liniger equation Eq. (47), with the kernel K given by Eq. (39). It takes the form

$$\rho(\lambda) - \frac{1}{2\pi} \int_{-\lambda_F}^{\lambda_F} d\mu \frac{2c\rho(\mu)}{(\lambda - \mu)^2 + c^2} = \frac{1}{2\pi}. \quad (\text{D1})$$

First we rescale variables to find

$$\rho(\tilde{\lambda}) - \frac{1}{2\pi} \int_{-1}^1 d\tilde{\mu} \frac{2\tilde{c}\rho(\tilde{\mu})}{(\tilde{\lambda} - \tilde{\mu})^2 + \tilde{c}^2} = \frac{1}{2\pi}.$$

If \tilde{c} is very small, then we use an approximation

$$\frac{1}{2\pi} \frac{2\tilde{c}}{\tilde{\lambda}^2 + \tilde{c}^2} \approx \delta(\tilde{\lambda}) + \frac{\tilde{c}}{\pi\tilde{\lambda}^2}.$$

This gives

$$\int_{-1}^1 d\tilde{\mu} \frac{\rho(\tilde{\mu})}{\tilde{\lambda} - \tilde{\mu}} = \frac{\tilde{\lambda}}{2\tilde{c}}.$$

The solution to this well known integral equation states

$$\rho(\tilde{\lambda}) = \frac{1}{2\pi\tilde{c}} \sqrt{1 - \tilde{\lambda}^2}, \quad (\text{D2})$$

or equivalently

$$\rho(\lambda) = \frac{\lambda_F}{2\pi c} \sqrt{1 - \frac{\lambda^2}{\lambda_F^2}}. \quad (\text{D3})$$

We emphasize that Eq. (D3) is only correct for $|\lambda| \lesssim \lambda_F$, and it definitely breaks down for λ close to the Fermi momentum. For example, taken naively Eq. (D3) predicts that $\rho(\lambda_F) = 0$. In truth, $\rho(\lambda_F)$ is not zero, but it is just much smaller than $1/c$.

Eq. (D3) can be used to compute the total density

$$D = \int_{-\lambda_F}^{\lambda_F} d\mu \rho(\mu) = \frac{\lambda_F^2}{4c}. \quad (\text{D4})$$

From here we can compute the Fermi velocity

$$v_F = \frac{D}{\frac{\partial D}{\partial \lambda_F}} = \frac{\lambda_F}{2}. \quad (\text{D5})$$

Notice that this is exactly half of the Fermi velocity in the strong interaction case. We can now find the chemical potential h using

$$\frac{\partial h}{\partial \lambda_F} = v_F, \rightarrow h = \frac{\lambda_F^2}{4}.$$

The excitation spectrum can be found by solving the integral equation for the excitations

$$\epsilon(\lambda) - \frac{1}{2\pi} \int_{-\lambda_F}^{\lambda_F} d\mu \frac{2c\epsilon(\mu)}{(\lambda - \mu)^2 + c^2} = \frac{\lambda^2}{2} - \frac{\lambda_F^2}{4}. \quad (\text{D6})$$

With the appropriate rescaling Eq. (75), with the rescaled $\epsilon(\lambda) = q^2 \tilde{\epsilon}(\tilde{\lambda})$, and by taking the limit of small c , we bring this integral equation to the form

$$\int_{-1}^1 d\tilde{\mu} \frac{\tilde{\epsilon}(\tilde{\mu})}{\tilde{\lambda} - \tilde{\mu}} = \frac{1}{2\tilde{c}} \left(\frac{\tilde{\lambda}^3}{6} - \frac{\tilde{\lambda}}{4} \right).$$

The solution to this equation reads

$$\epsilon(\lambda) = -\frac{\lambda_F^3}{6c} \left(1 - \frac{\lambda^2}{\lambda_F^2} \right)^{\frac{3}{2}}, \quad |\lambda| \lesssim \lambda_F. \quad (\text{D7})$$

For larger values of λ we can use the integral equation Eq. (D6) to find

$$\epsilon(\lambda) = \frac{\lambda_F \lambda}{2} \sqrt{\frac{\lambda^2}{\lambda_F^2} - 1}, \quad |\lambda| \gtrsim \lambda_F. \quad (\text{D8})$$

Notice that in the vicinity of $|\lambda| = \lambda_F$, both Eq. (D7) and Eq. (D8) break down. In particular, these expressions cannot be used to compute the Fermi velocity Eq. (D5)

simply by differentiating the energy ϵ with respect to the momentum at $\lambda = \lambda_F$.

It is also instructive to compute the physical momentum of the excitations k , using Eq. (55). For this purpose the phase shift $\theta(\lambda)$ can be replaced by $\pi \text{sign } \lambda$, which gives

$$\begin{aligned} \tilde{k} &= \tilde{\lambda} + \frac{\tilde{\lambda}}{2\tilde{c}} \sqrt{1 - \tilde{\lambda}^2} + \frac{\arcsin \tilde{\lambda}}{2\tilde{c}}, \quad |\tilde{\lambda}| \leq 1, \\ \tilde{k} &= \tilde{\lambda} + \frac{\tilde{\lambda}}{4\tilde{c}}, \quad |\tilde{\lambda}| > 1. \end{aligned} \quad (\text{D9})$$

Here $\tilde{k} = k/\lambda_F$.

Finally, the Luttinger parameter of the Bose gas is given by

$$g = \frac{\pi D}{v_F} \approx \pi \sqrt{\frac{D}{c}}. \quad (\text{D10})$$

The second equality is valid only in the limit $g \gg 1$. The Luttinger parameter at small c can also be derived with the bosonization techniques [16], and the answer coincides with Eq. (D10).

APPENDIX E: MOLECULAR DENSITY AND THREE-BODY PROCESSES

We would like to give an estimate of what percentage of the atomic wave function is concentrated inside the molecules. We will do it by directly calculating the wave function of the single-particle Fano Anderson model Eq. (20). Indeed, its Hamiltonian is quadratic, so it can be diagonalized by the appropriate rotation of the operators a, b . Its eigenstates at the energy ϵ can be constructed by writing

$$\psi(\epsilon) = c_0 b^\dagger |0\rangle + \sum_k \alpha_k a_k^\dagger |0\rangle.$$

where c_0 and α_k satisfy, curtesy of Eq. (20), the following equations (L is the size of the system)

$$\begin{aligned} \epsilon_0 c_0 + \frac{g}{\sqrt{L}} \sum_k \alpha_k &= \epsilon c_0, \\ c_0 \frac{g}{\sqrt{L}} + \epsilon_q \alpha_q + \frac{c}{L} \sum_k \alpha_k &= \epsilon \alpha_q. \end{aligned}$$

It follows that

$$\alpha_q = \frac{c}{g\sqrt{L}} \frac{\epsilon - \epsilon_1}{\epsilon - \epsilon_q} c_0,$$

while the energy level ϵ satisfies

$$\frac{c}{L} \sum_q \frac{\epsilon - \epsilon_1}{\epsilon - \epsilon_q} = \epsilon - \epsilon_0. \quad (\text{E1})$$

Here ϵ_1 is given, as before, by Eq. (25), and $\epsilon_q = q^2/(2m)$.

The normalization condition for the wave function states

$$c_0^2 + \sum_q \alpha_q^2 = c_0^2 \left(1 + \frac{c^2}{g^2 L} \sum_q \left(\frac{\epsilon - \epsilon_1}{\epsilon - \epsilon_q} \right)^2 \right) = 1.$$

Thus the condition that the particle spends most of its time outside the molecular state, created by b^\dagger , can be formulated as follows

$$\frac{c^2}{g^2 L} \sum_q \left(\frac{\epsilon - \epsilon_1}{\epsilon - \epsilon_q} \right)^2 \gg 1. \quad (\text{E2})$$

We would like to apply this condition to make sure that atoms spend only a small fraction of their time bound into molecules in the regimes of interest in this paper.

Consider first the case of small c . At densities up to the critical density Eq. (4), the particles from the Fermi sea, having momenta from $-\lambda_F$ to λ_F , are not in resonance with each other, so their quasistationary bound states can be completely neglected. Suppose we add one more particle. Its spectrum is shown on Fig. 10. If its momentum is of the order of $2\lambda_0$, the particle is in resonance with particles in the Fermi sea and spends at least some of its time bound into a molecule. This corresponds to the local minimum in $\epsilon(\lambda)$ as shown on Fig. 10. In order to be able to trust the physics of Fig. 10, we need to verify that the condition Eq. (E2) holds for the majority of the two body processes between the particle with momentum close to $2\lambda_0$ and the particles in the Fermi sea.

We observe that at c small, essentially only one term with optimal q , where $\epsilon - \epsilon_q \sim c$, contributes to the sum in Eq. (E1). We can use that to estimate $\epsilon - \epsilon_q$ and

substitute into Eq. (E2), again retaining only one term in the sum. We find

$$\frac{L}{g^2} (\epsilon - \epsilon_0)^2 \gg 1.$$

This condition is clearly violated for the particles exactly at resonance, so that $\epsilon = \epsilon_0$. Yet we only need to check that this condition holds for the typical pair of particles, not just those which are exactly at resonance. The typical momentum difference for a particle at $\lambda = 2\lambda_0$ and a particle in the Fermi sea is given by $2\lambda_0 + \lambda_F$, and a typical energy is

$$\epsilon - \epsilon_0 = \frac{(\lambda_0 + \frac{\lambda_F}{2})^2}{2m} - \frac{\lambda_0^2}{2m} \sim c^{\frac{1}{3}} \epsilon_0^{\frac{5}{6}} m^{\frac{1}{6}}.$$

Here we used the estimate Eq. (5) for λ_F . Hence the criterion becomes

$$\frac{L}{g^2} c^{\frac{2}{3}} \epsilon_0^{\frac{5}{3}} m^{\frac{1}{3}} \gg 1.$$

Observing that $g^2 \sim c$ (due to ϵ_1 , defined in Eq. (25), being finite) we find that the above condition definitely holds at small c . Thus we proved that at small c , in the regime of interest to us where the density is of the order of Eq. (4), the particle spends the overwhelming majority of its time outside the molecular state.

The case of large c is somewhat harder to analyze as we do not have an analytic solution of this problem even with two-body interactions neglected. Nevertheless we expect the condition Eq. (E2) to hold as c is now large, and, unless the energy ϵ is exactly at resonance, the particle still spends most of its time outside the molecular state.

-
- [1] M. Girardeau, *J. Math. Phys.* **1**, 516 (1960).
[2] E. Lieb and W. Liniger, *Phys. Rev.* **130**, 1605 (1963).
[3] F. D. M. Haldane, *Phys. Rev. Lett.* **47**, 1840 (1981).
[4] B. Paredes, A. Widera, V. Murg, O. Mandel, S. Fölling, I. Cirac, G. V. Shlyapnikov, T. Hänsch, and I. Block, *Nature* **429**, 277 (2004).
[5] E. Timmermans, P. Tommasini, M. Hussein, and A. Kerman, *Physics Reports* **315**, 199 (1999).
[6] V. Gurarie and L. Radzihovsky, in preparation (2005).
[7] L. Radzihovsky, J. Park, and P. Weichman, *Phys. Rev. Lett.* **92**, 160402 (2004).
[8] D. E. Sheehy and L. Radzihovsky, *Phys. Rev. Lett.* **95**, 130401 (2005).
[9] E. Lieb, *Phys. Rev.* **130**, 1616 (1963).
[10] A notable exception to this is given by Eq. (1) if $\epsilon_0 - g^2/c = 0$. This corresponds to the binding energy of the molecules being exactly zero. Under these conditions, Eq. (13) is not applicable and in fact, $S(0) = 1$. We will not consider such situation in this paper, limiting ourselves to the Feshbach Hamiltonian satisfying Eq. (2).
[11] V. E. Korepin, N. Bogoliubov, and A. G. Izergin, *Quantum Inverse Scattering Method and Correlation Functions* (Cambridge University Press, Cambridge, UK, 1993).
[12] L. D. Landau and E. M. Lifshitz, *Quantum Mechanics* (Butterworth-Heinemann, Oxford, UK, 1981).
[13] U. Fano, *Phys. Rev.* **124**, 1866 (1961).
[14] G. D. Mahan, *Many-Particle Physics* (Kluwer Academic/Plenum Publishers, New York, NY, 2000), chap. 4.2, p. 207.
[15] A. C. Hewson, *The Kondo Problem to Heavy Fermions* (Cambridge University Press, Cambridge, UK, 1993), chap. Appendix A, p. 363.
[16] M. Cazalilla, *J. Phys. B: At. Mol. Opt. Phys.* **37**, S1 (2004).